2023

Effect of Estrogen on Chondrogenesis in Female Articular Chondrocytes

Ebony R. Parsons
University of Central Florida

EFFECT OF ESTROGEN ON CHONDROGENESIS IN FEMALE ARTICULAR CHONDROCYTES

by

EBONY PARSONS

A thesis submitted in partial fulfillment of the requirements
for Honors in the Major program in Biomedical Sciences
in the College of Medicine
and in the Burnett Honors College
at the University of Central Florida
Orlando, Florida

Fall Term, 2023

Thesis Committee
Chair: Thomas Kean, PhD
Co-Chair: Alicia Hawthorne, PhD
Member: Kyle Rohde, PhD

ABSTRACT

As women age and transition into menopause they face a higher risk of developing osteoarthritis leading to total joint replacements. Estrogen is the primary female reproductive hormone. As a woman approaches menopause, estrogen production decreases by 100-fold. Previous research has shown that Estrogen Replacement Therapy (ERT) reduced joint replacements in post-menopausal women. However, there is a lack of research surrounding ERT's effect on chondrocyte proliferation and extracellular matrix production, particularly 3D culture extracellular matrix production. Chondrogenesis is a process of skeletal development resulting in the formation of cartilage. Chondrocytes, derived from mesenchymal progenitors, serve as the fundamental cellular component in the development of articular cartilage, facilitating smooth joint movement. This thesis examines female articular cartilage in both 2D growth assessment and using 3D aggregates with and without arthritis-like inflammatory conditions. Estrogen seems to have minimal effect on growth, metabolic activity, and extracellular matrix production. Healthy and pre-exposed osteoarthritic cartilage donors indicate some variability within the data. Overall, this project allowed us to further elucidate the mechanism of estrogen hormone replacement therapy utilizing healthy and osteoarthritic samples.

ACKNOWLEDGEMENTS

The completion of these experiments could not have been possible without the expertise of Dr. Thomas Kean, my thesis chair. I would also like to thank Dr. Alicia Hawthorne, my co-thesis chair and Dr. Kyle Rohde, committee member, for continuously offering invaluable feedback. Furthermore, thank you to the Gift of Hope program at Rush University and Dr. Chubinskaya for the generous donation of the healthy talus tissue utilized in our experiments.

Last but not least, I would like to thank my fellow lab members who willingly performed some of my lab tasks in my absence and my mother, Jessica Weinhauer, for supporting me throughout this process.

TABLE OF CONTENTS

LIST OF FIGURES

LIST OF TABLES

1. INTRODUCTION

1.1 Chondrogenesis and Aging

The formation of cartilage and bone template occurs during the first stage of skeletal development, known as chondrogenesis [1]. Cellular interactions, growth factors, and environmental factors can either suppress or initiate signaling pathways between cells. This is important to note as both cell growth, and the extra cellular matrix production can be altered by these conditions. Chondrogenesis occurs following the condensation of the mesenchyme, which results in the formation of collagens I, II, III, V, IX and XI [2, 3]. Chondrocytes, the only cell type in cartilage, arise from mesenchymal stem cell progenitors to make cartilage and templates for developing bone [1]. Following the chondrogenesis process, chondrocytes can form articular cartilage, undergo proliferation, or apoptosis. The apoptotic process leads to endochondral ossification where the hypertrophic chondrocytes, descendants of proliferating chondrocytes, are replaced by bone [2].

Literature suggests that chondrocytes begin to deteriorate with age, also known as senescence [4, 5]. As chondrocytes age, they become smaller, less functional, and their activity begins to decline overall [5]. Martin and Buckwalter (2003) measured the cell senescence markers: β-galactosidase expression, mitotic activity, and telomere length; leading to the discovery that β-galactosidase expression increased with age, while mitotic activity and telomere length decreased [4]. Overall, the results support previous *in vivo* studies that chondrocyte senescence contributes to the decreased efficacy of cartilage repair [4]. Barbero et al. (2004) investigated how aging

affects human chondrocyte yield, proliferation, chondrogenic capacity, under specific growth factor supplementation using female and male cadavers ages 20 to 91 [5]. Using a cell culture technique, the results for cadavers without the calreticulin growth factor supplementation showed cell yields were similar in cadavers up to 40 years old and lower in cadavers above 40 [5]. There was a significant decrease in cell yield from the 30-year-old age group (7.9 million cells/ tissue) to the 40-year-old group (4.5 million cells/gram tissue) [5]. Although male and female donors were used, the researchers did not study sex differences [5].

1.2 Estrogen and Aging

Estrogen is the primary female reproductive hormone and is responsible for the control of the reproductive system, in addition to other functions that occur from puberty onwards [6]. Estrogens refer to several female hormones including estrone (E1), estradiol (E2), estriol (E3), and estetrol (E4) [6]. These estrogens are synthesized in the ovaries and adrenal glands which will produce hormones in response to signals from the brain, more specifically signals from the pituitary gland [6].

1.3 Physiological Effects of Estrogen

Estradiol (E2) is the primary gonad hormone in premenopausal women. Following menopause, estradiol levels decrease to less than 20 pg/ml from the normal premenopausal levels of 40-400 pg/ml [7]. Estriol (E3) and estetrol (E4), more often manifest at high levels in pregnant women and low levels in nonpregnant women. There are three important estradiol concentrations throughout a woman's life: 10^{-7} M (pregnancy), 10^{-9} M (ovulation), 10^{-11} M (menopause) [19].

Similar to all steroid hormones, once the estrogens reach their target organ, estrogen will diffuse into the cells and attach to an estrogen receptor [Fig. 1].

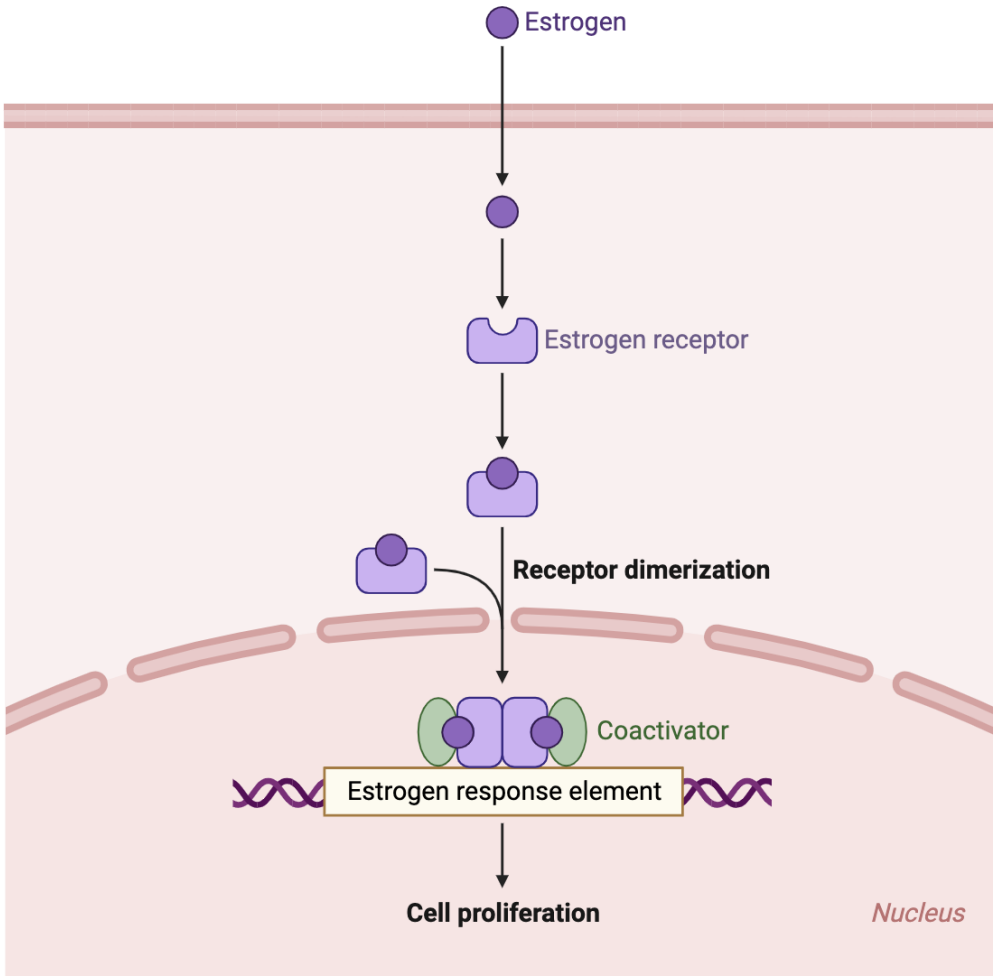

Figure 1 - Estrogen Mechanism. Estrogen (E2) diffuses passively into the target cell and binds to an estrogen receptor in the cytoplasm. The estrogen receptor then dimerizes and enters the nucleus inducing cell proliferation. Created with Biorender.com

ERα and ERβ are considered to be the plasma membrane receptors for estrogen [8]. ERα and ERβ are found to exist as a dimer in the cytoplasm, which affects cell physiology due to the structure supporting the binding of the extracellular messenger to the cell surface receptor. This action will affect the physiological action initiated by estrogen in the target tissue.

Within the reproductive organs, estrogen stimulates the growth of smooth muscle and the development of the epithelial lining of the uterus and vagina [7]. This is significant to note because it highlights the direct impact estrogen has on the regulation of the menstrual cycle in premenopausal women.

1.4 Estrogen Receptors

In 1958, Elwood Jensen et al. discovered that due to the binding of estradiol-17β (E2) to cells found in the uterus, noting that the effects of estrogen must be mediated by a receptor protein, ERα [6, 39]. Jensen et al. found a target for drug action, otherwise known as the estrogen receptor. In 1996, ERβ was the second cloned ER [40].

Estrogen receptors have genomic and nongenomic signaling effects [10]. The genomic effects are known as classical signaling, where the estrogen binds to the intracellular ER's which become translocated to the nucleus and bind to estrogen response elements. Nongenomic effects are known as nonclassical signaling, where protein-protein interactions take place rather than the direct binding to the estrogen response elements [10]. For instance, in nonclassical signaling, genomic signaling has been indirectly modulated by ERα and ERβ through their interactions with transcription factors that activate protein-1 (AP-1) and stimulate protein-1 (SP1). Ushiyama et al. (1999) investigated the expression of estrogen receptors ERα and ERβ in human chondrocytes using both male and female donors [9]. The study concluded that both estrogen receptors were more expressed in males than females [9]. Women expressing lower levels of ERα and ERβ could suggest a potential reasoning as to why they experience increased estrogen fluctuations during their life when compared to men [9]. ERα and ERβ bind estrogen and

facilitate the normal biological function of estrogens, thus having lower levels of these receptors may lead to decreased control of estrogen [36].

1.5 The Menstrual Cycle

The period of time when menstruation ceases is known as menopause. During a normal menstrual cycle, the ovaries will produce estrogen and progesterone. Both promote the maturation and release of an egg within the ovaries [3]. During menopause, estrogen decreases significantly which correlates with a decrease in chondrocyte production (see the *Chondrocytes and Estrogen* section 1.9). The pituitary gland secretes follicle-stimulating hormone (FSH) which promotes egg maturation within the follicles, and luteinizing hormone (LH) which causes ovulation in women as explained in *Figure 2*.

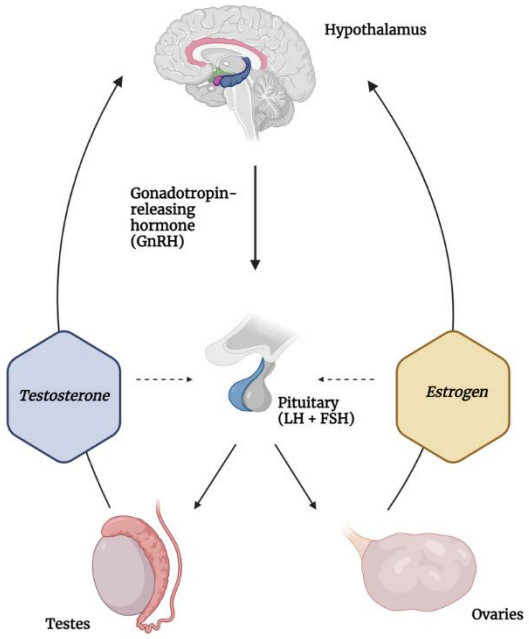

Figure 2 - Luteinizing Hormone (LH) & Follicle-Stimulating Hormone (FSH) Pathway. The principal regulator of LH and FSH secretion is the gonadotropin-releasing hormone (GnRH). The GnRH stimulates the secretion of LH, stimulating estrogen and progesterone in women and testosterone in men [11]. Created with Biorender.com

Once a woman begins menopause both FSH and LH will be secreted at higher levels to compensate for the lack of estrogen until egg fertilization is unsustainable and conception cannot occur. Elevated levels of FSH associated with estrogen decrease may also pose a damaging effect on cartilage tissues leading to knee osteoarthritis [12]. Phosphoinositide 3-kinase (PI3K)/PI3K, p-AKT/AKT and p-nuclear factor kappa B (NF-κB)/NF-κB have been found to be involved in the degeneration and destruction of osteoarthritic articular cartilage [12]. It is proposed that high FSH levels are associated with increased cartilage degradation in postmenopausal women due to high FSH levels promoting the PI3K/AKT/NF-κB pathway in women aged 50-60 years when FSH is at its peak [12].

1.6 Perimenopause

Perimenopause is the precursor to menopause and marks the transitional time until a woman experiences the final menstrual period (FMP). Data suggests perimenopause can begin up to 8 years before the FMP [14]. Around the average age of 47, women begin to experience a gradual onset of hormonal fluctuations, indicative of perimenopause [14]. The perimenopausal transition can be divided into early and late phases with several hallmark symptoms which depend on a woman's cycle and ovarian endocrine function [15]. Early perimenopause is characteristic of more than seven days difference from the normal cycle. A late perimenopause diagnosis is associated with more than two missed cycles or less than 60 days (about 2 months) after the onset of amenorrhea (absence of menstruation).

During the perimenopausal period, menstrual cycles become irregular, and women begin to miss several periods; however, pregnancy is still possible. As women approach their late thirties, the ovaries begin to produce less estrogen and progesterone. The pituitary gland then produces increased levels of LH and FSH due to ovarian decline. Ultimately, the production of these hormones and egg maturation can no longer be maintained, leading to complete menopause [15].

1.7 Menopause

Menopause is clinically defined as the complete cessation of menstruation in women. Menopause follows perimenopause and involves an extreme decrease in oocytes and a complete loss of gonadal steroids [16]. In the United States, the average age of menopause onset is 51 [18]. A woman has officially transitioned into menopause once she has experienced 12 months of

amenorrhea, the absence of menstruation [17]. Similar to perimenopause, there are two transition periods during menopause: early and late. The transitional phases have both menstrual cycle and endocrine system characteristics [16].

Early menopause characteristics include a minor increase in the prevalence of common menopausal symptoms, but deviations in the menstrual cycle are minimal [31]. Women will also have at least 1 menstrual cycle within the previous 3 months. Hypothyroidism is also commonly seen as hormone secretion increases rapidly to keep up with a failing reproductive system and levels of triiodothyronine (T3) and thyroxine (T4) begin to decrease [31]. T3 and T4 are important in the regulation of weight, energy levels, and metabolism. Late menopause characteristics include the decline of estrogen production due to the ovaries being unable to adapt to the changes in ovarian and pituitary hormone production. Bone mineral loss is also prevalent, potentially leading to deficient support of the articular cartilage surface [31]. Furthermore, there will be an increase in the severity of symptoms seen in perimenopause [31].

Menopause is the final stage of ovarian physiology due to the complete cessation of reproductive function [16]. As previously mentioned, the menopausal transition ends following the FMP. The Daily Hormone Study investigated women's menstrual cycle hormones as they approached menopause [17]. A total of 511 premenopausal and early perimenopausal women enrolled with the target age being around 10 years before menopause. This novel study collected daily samples for a complete menstrual cycle or 50 days (about 1 and a half months) and detailed hormone patterns associated with small increases in LH and FSH over time. The sampling was repeated

once a year until the FMP or at the most 10 years. The stability of menstrual cycles persisted until three years prior to the onset of the final menstrual period (FMP), which coincided with a surge in gonadotropins. This surge stimulated the pituitary gland to produce higher levels of luteinizing hormone (LH) and follicle-stimulating hormone (FSH), resulting in elevated levels of estradiol until the onset of menopause. Progesterone decreases over time, allowing estrogen to take over, or be unopposed, which can cause irregular bleeding and ovarian cancers just before menopause [17].

1.8 Stages of Reproductive Aging Workshop

The Stages of Reproductive Aging Workshop (STRAW) was developed in 2001 as a staging criterion for ovarian aging and is divided into three phases [19]. The first phase is the Reproductive Phase, which includes the following stages: -5 (early), -4 (peak), -3 (late). Stage -3 is characterized by regular menstrual cycles with increasing FSH levels. The second phase is the Menopausal Transition, which includes the following stages: -2 (early), -1 (late). Stage -2 is characterized by variability in menstrual length and increased levels of FSH. Stage -1 is characterized by skipped cycles or onset of amenorrhea for at least 60 days (about 2 months) and continued increase of FSH. Stage 0 marks the Final Menstrual Period just before post menopause. The third phase is Postmenopausal, which includes the following stages: +1 (early), +2 (late). In 2011, changes were made to the STRAW criteria to improve patient assessments (Table 1.) [16].

Table 1. STRAW Improvement Criteria [16].

Reproductive Stage	Menopausal Transition Stage –2 (early)	Menopausal Transition Stage –1 (late)	Postmenopausal Stage +1 (early)
1. Cycles are regular or become slightly irregular 2. Normal to variable FSH levels 3. Low ovarian reserve (egg count)	1. ≥ 7-day fluctuation in cycle length 2. Evident fluctuation in FSH 3. Low ovarian reserve	1. Cycles occur ≥ 60 days between each other 2. High FSH levels 3. Low ovarian reserve	1. Extreme decrease in ovarian reserve, sometimes undetectable

The STRAW criteria are still considered the gold standard for characterizing reproductive aging through menopause with Stage 0 being the FMP.

1.9 Chondrocytes and Estrogen

When chondrocytes age, cartilage degenerates and senescence occurs [20]. Estrogen can affect both articular cartilage and MSCs (Mesenchymal Stromal Cells) through the estradiol (E2) mechanism which affects the binding of ERs and the expression of proteins, such as X-ray Repair Cross Complementing 5 (XRCC5, co-ordinates DNA repair) and NAD-dependent deacetylase sirtuin-1 (SIRT1, prevents apoptosis and senescence) [20].

Furthermore, Liang et al., delved deeper into the mechanism of miR-140 in E2 regulated matrix metalloproteinase-13 (MMP-13) [26]. MMP-13 is an enzyme present in cartilage extra-cellular matrix responsible for degradation [26]. Liang et al. obtained primary human chondrocytes, the cells that produce and maintain the extracellular matrix of cartilage, from female patients undergoing total knee replacement surgery. Cells were grown in monolayer and treated with estrogen and IL-1β. The chondrocytes were cultured and examined using immunofluorescence microscopy, PCR, and Western blotting. IL-1β induced the expression of MMP-13 leading to induced extra-cellular matrix degradation, while 10^{-8} M E2 was used after treatment to determine effects. The study concluded that IL-1β-induced expression of MMP-13 and miR-140 expression is blocked by E2 regulating miR-140 and altering MMP-13 activity [26]. This is important to note as this indicates E2 reduces cartilage degradation by downregulating MMP-13 activity (≤24h). Thus, providing additional evidence regarding utilizing estrogen HRT as a treatment to prevent OA.

The telomeric effect of differing estrogen concentrations (10^{-7} M, 10^{-9} M, 10^{-11} M*)* on perimenopausal and postmenopausal human mesenchymal stem cells and chondrocytes was also investigated in 2D culture for eight months [20]. Shortening of the telomere is regarded as a reliable indicator leading to the onset of cell senescence. The experimental E2 concentrations mimicked estrogen levels during a woman's life; 10^{-7} M (pregnancy), 10^{-9} M (ovulation), 10^{-11} M (menopause). The study concluded that telomeres were longer with concentrations of E2 at 10^{-7} M and 10^{-9} M but that cell proliferation was unaffected [20].

Gender differences related to chondrocyte repair and cartilage reduction are evident in literature [31, 32]. A study from 2004 investigated the different physiological responses of articular cartilage to estradiol. Estrogen along with G-protein and phosphatidylinositol-specific phospholipase C activate protein kinase C (PKC) in many different cell types [32]. When chondrocytes were treated with 10^{-9} M, 10^{-8} M, and 10^{-7} M estradiol, the signaling activity of PKC in female chondrocytes significantly increased [32]. Contrarily, male chondrocytes showed no response in PKC activity at those concentrations. The study concluded that female chondrocytes were responsive to estradiol while male chondrocytes were not [32]. A review from 2023 compiled the various findings of knee variation, sex hormones' effect on cartilage, and cartilage degeneration and regeneration with a focus on stem cells in men and women [31]. Patel et al. concluded that women have an increase in inflammatory biomarkers, such as leptin [31]. In addition, women also have an increased loss of glycosaminoglycans within the extracellular matrix when compared to males. These papers are important to mention as both highlight the need to investigate cartilage responses in women. Thus, postmenopausal women have an increased risk of cartilage loss and OA when compared to men of the same age.

1.10 Hormone Replacement Therapy

The goal of estrogen HRT is to replace estrogen to diminish menopausal symptoms such as vasomotor symptoms, urinary complaints, and vaginal atrophy [21]. Studies suggest estrogen hormone replacement therapy to be an effective joint-protecting treatment for women transitioning into menopause [24, 25]. In addition, HRT also has been shown to decrease joint pain and arthralgia symptoms associated with aging [24]. In 1991, the Women’s Health Initiative

conducted two randomized controlled trials of unopposed estrogen and opposed estrogen HRT in postmenopausal women aged 50-79 [25]. In unopposed estrogen, progestin is absent or at low levels thus causing estrogen dominance. In opposed estrogen, progestin is present (0.625 mg of conjugated equine estrogen plus 2.5 mg of medroxyprogesterone acetate) [25]. The results concluded that HRT was effective in controlling vasomotor symptoms, sleep fluctuations, and vaginal dryness associated with the menopausal transition. Of the women receiving HRT, 47% reported joint pain and arthralgia improvement [25]. Rousseau et al. (2001) reviewed the effects of estrogen HRT in menopausal women [21]. The review concluded that the greatest effect of HRT is the decrease in osteoporosis, a loss of bone mass associated with joint pain, arthritis, and cartilage damage [21]. Cirillo et al. also concluded in their review that women with long-term exposure to HRT during perimenopause experienced a protective effect [24].

Wluka et al. (2001) studied menopausal women with long-term (> 5 years) estrogen HRT exposure. The study included 81 women, 42 of whom had long-term exposure to HRT, while 39 women acted as the control who never used HRT [22]. The results showed that, upon using estrogen HRT, there was an increase in total levels of tibial cartilage (2.98 mm HRT vs 2.75 mm control) [22]. This suggests that estrogen HRT may prevent the loss of articular cartilage in this area.

In 2006, a study done by the Women's Health Initiative investigated the effects of estrogen and progestins, which is a synthetic form of progesterone, on joint health in women aged 50-79 with a risk of hip or knee arthroplasty, a procedure done to restore joint function. The results

concluded that HRT positively influenced joint health and had a protective effect on the cartilage in women at risk of OA and arthroplasty [24]. Although there is ample support that suggests estrogen HRT protects cartilage, our hypotheses are that: estrogen will increase chondrocyte proliferation rate, increase extracellular matrix production and protect the extracellular matrix from inflammatory degradation *in vitro*.

2. METHODS

2.1 Determine the Effect of Estrogen Supplementation *In Vitro* on Human Chondrocyte Proliferation

2.1a Cartilage Dissection

Chondrocytes utilized in this study were obtained either from previously isolated cryopreserved stocks or isolated from ankle (talus) joints. Talus cartilage was dissected from three Gift of Hope (Rush University) human female donors and cryopreserved chondrocytes were isolated from three osteoarthritic female donors undergoing total knee replacement. Tissue obtained through the Gift of Hope program received approval from the Institutional Review Board through the Office of Research Affairs at Rush University Medical Center. UCF IRB deemed the work within this thesis as Non-Human Research. The tissue from Gift of Hope was initially assessed before dissection based on the degree of articular cartilage damage (Collin's grade) [40]. Cartilage showing minimal signs of damage (Grade 1) was utilized (Fig. 3) [29]. Cartilage with obvious surface fissures (Grade 2) were not used in the experiments but frozen down after resuspension in FBS containing DMSO (5%), see *Figure 4*.

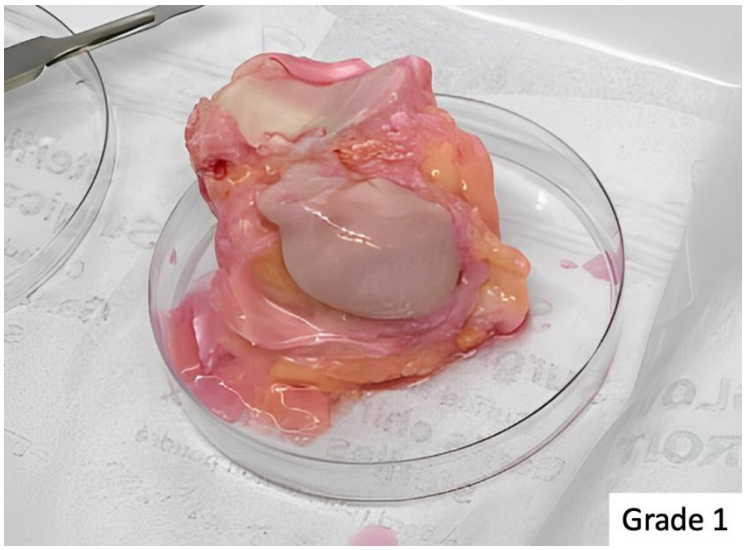

Figure 3 - Grade 1 Talus.

Figure 4 - Grade 2 Talus. Obvious surface fissure on the cartilage.

To isolate chondrocytes dissected from talus joints, the tissue was stored briefly (<8h) in room temperature chondrogenic bioreactor media (93.24% DMEM-HG, 1% penicillin/streptomycin,

1% ITS + premix, 0.5% fungizone, 1% 10^{-5} Dexamethasone, 1% 100X GlutaMax, 1% 100X MEM NEAA, 0.26% 50mM ascorbate-2-phosphate, and 1% 100 mM sodium pyruvate) to improve cell yield and time efficiency [27, 37]. Forceps and a scalpel blade were utilized to remove excess tendon, fat, muscle, and tissue. Following this, the cartilage tissue was dissected from the bone, which was then minced into smaller pieces. These fragments were digested with hyaluronidase (660U/mL, Sigma) for 30 minutes, 37°C, and centrifuged for 1 minute at 100 RCF. A second digest was then performed, wherein cartilage was digested in type II collagenase (583 U/mL, Worthington Biochemical Corp.) for a 12-hour incubation on a nutating rocker at 37°C. Following the digests, the cell slurry was removed from the incubator and filtered through a 70-μm nylon mesh (Biologix) into Falcon tubes. Subsequently, the tubes were centrifuged (690 RCF for 10 minutes). To count the cells, Cytosmart (Corning) automated cell counter was used.

Collins grade 2 tissue was frozen down for future use. DMSO (5%) was added to each Falcon tube containing the FBS (95%) and the resuspended cells. The solutions were then added into cryovials (1ml) and subsequently frozen down using a controlled rate freezing container (Nalgene® Mr. Frosty). Table 2 organizes all six biological replicates utilized and separates them based on whether they were cryopreserved or isolated from tissue donated to the Gift of Hope program (Dr. Chubinskaya, Rush University) [37]. For each experiment, all donors were separated into different plates and were never combined.

Table 2 - Donor Organization.

Cryopreserved (osteoarthritic), knee	Fresh, Gift of Hope (healthy), talus
1. 003-2016 (age/race/ethnicity: unknown) 2. 011-2016 (age/race/ethnicity: unknown) 3. 037-2018 (age: 76, race/ethnicity: unknown)	1. 7782 (age: 56, Caucasian) 2. 7783 (age: 51, Hispanic) 3. 7784 (age: 64, Caucasian)

2.1b Chondrocyte Isolation

Cryovials containing frozen chondrocytes were warmed until most of the ice was melted. Thereafter, 10 ml of growth media was added (10% FBS, 1% penicillin/streptomycin, 89% DMEM-LG/Ham's F12 in a 1:1 ratio). Once the frozen chondrocytes were thawed, they underwent centrifugation (500 RCF, 5 minutes) and were resuspended in 2ml of growth media. Trypan blue and the resuspended cell slurry were pipetted onto a hemocytometer and cell density was counted using CytoSmart (Corning). Chondrocytes from the Gift of Hope donors and frozen chondrocytes were then seeded onto synoviocyte matrix flasks (SCM flasks) at ~ 6,000 cells/cm^2 and fed on day 2 then every 3-4 days until they reached 95% confluency (5-10 days), as demonstrated in *Figure 5* [28, 33, 34, 41, 42].

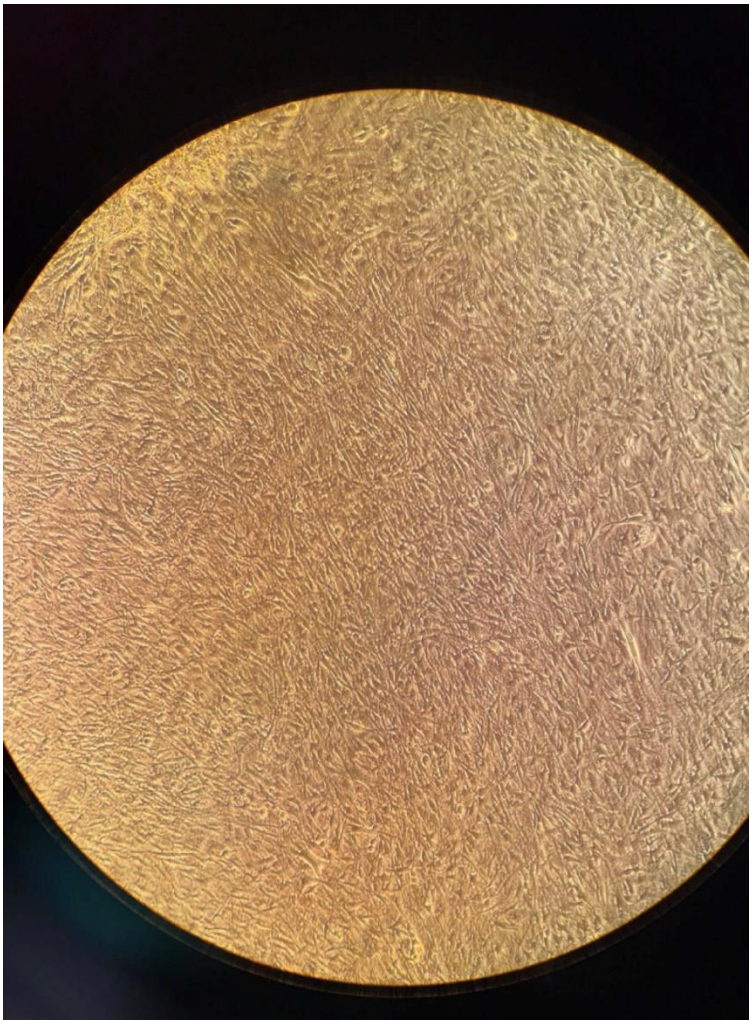

Figure 5 - Example of 95-100% confluency.

2.1c Formatting of Chondrocytes for Chondrogenic Assay

Basal chondrogenic media containing no estrogen treatment was split into Falcon tubes per condition and donor. The cells were treated with the following concentrations of E2: 10^{-7} M (pregnancy), 10^{-9} M (ovulation), 10^{-11} M (menopause) [19]. Growth media was also made (44.5% DMEM-LG, 44.5% Ham's F-12, 10% charcoal stripped FBS (to remove estrogen), 1% penicillin/streptomycin). Estradiol was added to growth media to give the same 10^{-7} M, 10^{-9} M, and 10^{-11} M concentrations. TGFβ1 (10 μg/ml) was added to the chondrogenic media following

the first experiment to improve cell differentiation due to low levels of GAG and type II collagen typical of human chondrocytes without TGFβ1.

Media was removed from the T175 synoviocyte matrix flasks following checking the chondrocytes under the microscope to ensure confluency. The chondrocytes were rinsed with PBS and subsequently removed. Trypsin-EDTA (5 ml) was added into the flask to cover the cell surface. The flask was incubated (5 min, 37°C) to ensure the cells lifted off the surface. Growth media (6 ml) was added to neutralize the trypsin and rinse the cells. The cell slurry was transferred into a 15 ml Falcon tube and centrifuged (500 RCF, 5 minutes) to form a pellet. The supernatant was removed, and the pellet was resuspended in 2 ml chondrogenic media. Trypan blue (20 µl) and the cell slurry (20 µl) were mixed then pipetted into the hemocytometer and counted using CytoSmart. The cell suspension contents from the Falcon tubes were then seeded into 96-well non-adherent round bottom plates to form 3D aggregates 50,000 cells/aggregate, see *Figure 6.* An automated protocol (OT2-Opentrons) was used to disperse the media and resuspended cells into the growth and pellet plate, respectively. Deep well plates were used to contain stocks of the growth and chondrogenic media feeding which was organized utilizing the Opentron. The cells were imaged and fed every 2-3 days until the end of chondrogenesis (day 22) [27, 28]. Half of the aggregate plate was treated with IL-1β *in vitro* on day 10 to determine if chondrogenesis was affected. IL-1β was used at a final concentration of 125 pg/ml, added to cartilage aggregates using the Opentron. IL-1β was added to the same wells in the deep well plate containing the chondrogenic media used to feed the cells at 125 pg/ml IL-1β from day 10 onwards.

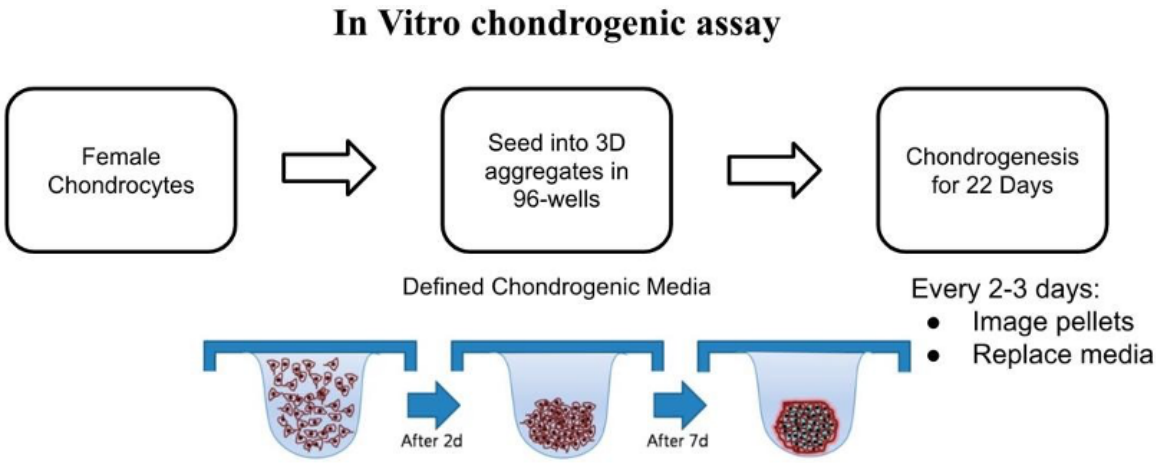

Figure 6 - In Vitro Chondrogenic Assay Process.

2.1d Formatting of Chondrocytes for Proliferation Assessment

Simultaneously with seeding for assessment of chondrogenesis, the chondrocytes were formatted into flat bottom 96-well cell culture plates to assess proliferation. The cells were treated with the same 3 concentrations of estradiol and a 0-estradiol control.

2.1e Resazurin Assay

Metabolic activity which is affected by cell number and viability was monitored using resazurin (TCI Chemicals). Resazurin (diluted 1:9 with PBS) was administered to the flat bottom, cell-adherent growth plate using the Opentron and incubated for three hours. After the incubation, resorufin fluorescence (the metabolic reduction product of resazurin) was analyzed (Biotek Synergy H1, excitation wavelength: 535 nm, emission wavelength: 588 nm).

2.1f Hoechst Staining

Cell proliferation was assessed using automated cell counting through nuclei labeling with Hoechst, see *Figure 6*. Hoechst dye (25 µl of 10 mg/ml in DMSO) was diluted with 225 µl PBS. An Opentron protocol was utilized to add the Hoechst to the designated wells within the growth plate for analysis (Biotek Synergy H1) to give a final concentration of 10 µg/ml in the well.

2.2 Determine the Effect of Estrogen Supplementation on Chondrocyte Extracellular Matrix Production

2.2a Aggregate Size Analysis

Aggregate size was analyzed using a Batch Measure plugin within the ImageJ program. Images of the 3D aggregates were taken every 2-3 days until day 22. The images collected were analyzed by ImageJ which produced results and summary data. The data was copied and pasted into Excel and each well was labeled with a specific estrogen concentration, area determined by ImageJ, replicate number per well (8-9 technical replicates), and day of chondrogenesis [37]. A pivot table was created from the data and uploaded into Prism to produce coherent graphs for visualization.

2.2b Histology Embedding and Sectioning

Following the three-week culture period, aggregates were separated into histology and biochemical samples. Formalin (500 µl) was added into eight Eppendorf tubes and each histology sample was fixed per condition overnight. The following day, formalin was replaced with 1 ml of PBS. To prepare the aggregates for paraffin embedding, 1% agarose in PBS was

melted and placed into a bead warmer to maintain a liquid consistency. A disc of agarose (4mm) was made in a silicone mold on a glass slide on a slidewarmer at 45°C and the aggregate placed in the agarose. The slide was then removed from the slidewarmer, allowed to cool and then the agarose disc containing the cartilage aggregate placed in histology cassette. Labeled cassettes were placed into a beaker ethanol (70%, stored at 4°C). Once ready to process, the samples were then embedded into paraffin wax using the Leica Biosystems Embedder.

After embedding the cartilage into the wax, a water bath and slide warmer were heated in preparation for sectioning. Excess wax was trimmed from the blocks containing the aggregates. The sectioning blade was locked into the Leica Biosystems RM2125 RTS Microtome to prepare for sectioning. Samples were then trimmed and sectioned onto slides (5 μm). Aggregate presence was confirmed by placing the wax film ribbon into a warm water bath. Slides were tapped off with each added film to eliminate excess water then dried overnight at 37°C. Three slides were utilized per condition and labeled for histology. Slides were warmed at 45 °C (5-20 min) before deparaffinization and staining.

2.2c Histology Staining

The extracellular matrix production and location was assessed histologically using safranin-o to determine glycosaminoglycan deposition [Figure 8]. All histology samples were qualitatively evaluated for GAG deposition. Paraffin embedded samples were sectioned (5 μm) onto slides and deparaffinized (xylene, 100% EtOH, 90% EtOH, 70% EtOH, H2O). Following deparaffinization, the slides were stained with Weigert's Iron Hematoxylin, destained with acid

ethanol then subsequently stained in Fast Green FCF (VWR/Alfa Aesar). Once slides were stained in fast green, they were rinsed in 1% acetic acid, dehydrated (95% ethanol, 100% ethanol, xylene), and then cover slipped with cytoseal (Thermo Fisher).

In addition to safranin-o staining, immunohistochemistry for type II collagen expression was performed [Figure 13]. All histology samples were qualitatively evaluated for type II collagen deposition. After deparaffination, the slides were moved to a humidified chamber and the samples were surrounded using an ImmEdge™ Hydrophobic Barrier Pen (PAP pen). Samples were then incubated with PBS and Pronase (1 μg/ml, Sigma) then blocked with 3% BSA (BSA Fraction V, OmniPur). Primary antibody (Collagen type II 1:200, DSHB II-II6B3) in 1% BSA was added to all samples aside from the preselected control sample and incubated, without rinsing, overnight at 4°C. The following day, the samples were rinsed with PBS, blocked with 3% BSA, and incubated with a secondary antibody (Biotinylated horse anti-mouse 1:2000, Vector labs, BA-2000) for one hour. Samples were rinsed again with PBS, incubated with HRP-conjugated Streptavidin (Invitrogen #SNN1004) for 30 minutes, and subsequently incubated with VIP substrate for ten minutes. Following this procedure, the slides were exposed to a Fast Green Counterstain and cover slipped (Fast Green, Glacial Acetic Acid, 100% EtOH, 100% Xylene).

2.2d Biochemical Assays

DNA assays were performed to monitor DNA concentration to assess cell proliferation in the aggregate culture. Sample plates were taken from the freezer and thawed at room temperature.

Papain Buffer (100 µl of 25 µg/ml in 2 mM Cysteine) was added to each well. Plates were sealed with TempPlate® Rt Select Optical Film, silicone mats, aluminum plates clamped with binder clips, and set in a dry incubator (65°C) to digest overnight. Standards were made from Calf Thymus DNA (Sigma) diluted with Neutralized Papain Buffer (0-10 µg/ml). The standards were added alongside the digested aggregate samples in duplicate (technical replicate) to a Black 96-well plate (Costar®) [37]. Hoechst dye (100µl of 0.66 µg/ml in 0.2 M phosphate buffer pH 8) was added to each well using a multichannel pipette. The plate was read using the Biotek ® Synergy H1 plate reader (excitation wavelength: 365 nm, emission wavelength: 460 nm).

GAG assays were performed to assess aggregate glycosaminoglycan content containing Neutralized Papain Buffer and Chondroitin Sulfate (Seikagaku) in Eppendorf tubes. Each standard (0-120 µg/ml) and sample (5 µl) were pipetted onto a clear flat bottom plate in duplicate. DMMB reagent (195 µl of 17.6 µg/mL in glycine buffer pH 1.5) was added to each well with a multichannel pipette and immediately read on the plate reader.

Hydroxyproline (HDP) assays were also performed to assess total collagen content. Samples were split between the DNA and HDP assay. HDP samples were added to a V-bottom plate (50 µl). 6M HCl (200 µl) was added to each well and sealed with adhesive film to incubate overnight at 105° C in the fume hood. The following day, the plates were cooled to 70° C and centrifuged (500 RCF, 1 minute). Hydroxyproline standards (0-500 µg/ml) were made containing HDP (Sigma) and Papain Buffer then plated onto the V-bottom plate in duplicate (10 µl). Samples were left overnight to dry out (70°C). Once dried, 0.15 M $CuSO_4$ and 2.5 M NaOH (10 µl) was

added to each well, centrifuged (500 RCF, 1 minute), and incubated at 50° C for ten minutes. H_2SO_4 (40 µl) and 20 µl Ehrlich's reagent (400 mg 4- (dimethyl amino) benzaldehyde, 2.4 ml Isopropanol, 1.04 ml Perchloric acid, 0.56 ml water) was added to each well, incubated at 70° C for sixteen minutes, then cooled to room temperature. With 70 µl in each well, the samples were transferred from the V-bottom plate into a 96-well clear flat bottom plate. Absorbance was read using Biotek ® Synergy H1 plate reader (wavelength: 505 nm).

2.2e Statistical Analysis

All the data collected throughout each experiment was uploaded into excel. A pivot table was created from the data and subsequently uploaded into Graph Pad Prism. A two-way ANOVA analysis was conducted to provide *p* values for the day, dose, and interaction.

3. RESULTS

3.1 Determine the Effect of Estrogen Supplementation *In Vitro* on Human Chondrocyte Metabolic Activity and Proliferation

The samples were assessed for metabolic activity using resazurin, which is affected by both metabolic activity and cell number. As expected, metabolic activity increased over time in culture concomitant with increased cell number (Fig. 7). In general, irrespective of the specific donor, the presence of 0 nM estrogen yielded the least amount of metabolic activity, while in the absence of estrogen, represented by 1 nM, led to the highest level of metabolic activity. After conducting an analysis of the data from individual donors, it was observed that a concentration of 100 nM estrogen led to the least amount of metabolic activity in Donors 003-2016 and 011-2016 on the ninth day (Appendix A, Fig. 16, 17). However, conversely, within the same donors, a concentration of 0 nM estrogen led to the greatest stimulation of metabolic activity. These results were observed in the frozen chondrocyte samples obtained from individuals with osteoarthritis. Donor 7782, obtained from healthy talus cartilage, did not show significant differences between estrogen concentrations other than at day six (Fig. 19). Although Donor 7784 was omitted from Figure 6 due to a lab error resulting in two days of data instead of three with only the 1st data point being valid. While minimal differences were found, overall, a two-way ANOVA identified interaction, day, and dose were statistically significant at $p = 0.0005$, < 0.0001, and $= 0.0151$, respectively. A Dunnett's post-hoc test vs. control (0 nM) was conducted (Table 3). Only days 8 and 9 showed statistical significance compared with 0 nM. The estrogen concentration of 0.01 nM did not indicate significance until day 9 ($p < 0.0001$). On day eight, 1 nM and 100 nM estrogen had significantly lower metabolic activity vs. 0 nM. While all estrogen concentrations

(0.01 nM, 1 nM, and 100 nM) had significantly higher metabolic activity on day 9. Individual donor graphs for metabolic activity can be viewed in Appendix A.

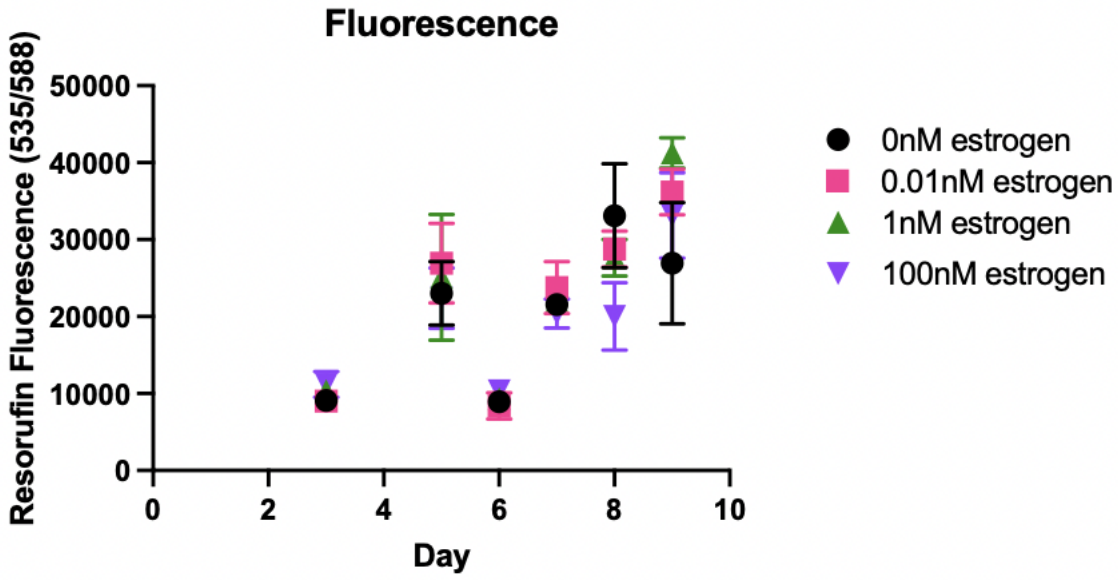

Figure 7 - Metabolic Activity of Chondrocytes During 2D Expansion Donor Average. Metabolic activity was assessed using resazurin for each condition. (Donors: 003-2016, 037-2018, 011-2016, 7782, 7783, Replicates per donor: ≥ 6)

Table 3 - Metabolic Activity Donor Average Post-hoc Test Results. Rows 1, 2, 3, 4, 5, and 6 represent days 3, 5, 6, 7, 8, and 9, respectively. Row 5 and 6 (Day 8 and 9) produced significant results.

Dunnett's multiple comparisons test	Predicted (LS) mean diff.	95.00% CI of diff.	Below threshold?	Summary	Adjusted P Value
Row 1					
0nM estrogen vs. 0.01nM estrogen	112.6	-4114 to 4340	No	ns	0.9998
0nM estrogen vs. 1nM estrogen	-1254	-5481 to 2973	No	ns	0.8223
0nM estrogen vs. 100nM estrogen	-2088	-6315 to 2138	No	ns	0.5062
Row 2					
0nM estrogen vs. 0.01nM estrogen	-3931	-8318 to 454.7	No	ns	0.0900
0nM estrogen vs. 1nM estrogen	-2100	-6487 to 2286	No	ns	0.5364
0nM estrogen vs. 100nM estrogen	592.0	-3794 to 4978	No	ns	0.9788
Row 3					
0nM estrogen vs. 0.01nM estrogen	545.9	-3681 to 4773	No	ns	0.9806
0nM estrogen vs. 1nM estrogen	-354.0	-4581 to 3873	No	ns	0.9945
0nM estrogen vs. 100nM estrogen	-1419	-5646 to 2807	No	ns	0.7645
Row 4					
0nM estrogen vs. 0.01nM estrogen	-2172	-6551 to 2207	No	ns	0.5050
0nM estrogen vs. 1nM estrogen	-494.9	-4725 to 3736	No	ns	0.9856
0nM estrogen vs. 100nM estrogen	1178	-3053 to 5409	No	ns	0.8488
Row 5					
0nM estrogen vs. 0.01nM estrogen	4335	-546.1 to 9215	No	ns	0.0937
0nM estrogen vs. 1nM estrogen	5481	599.9 to 10361	Yes	*	0.0233
0nM estrogen vs. 100nM estrogen	13083	8202 to 17963	Yes	****	<0.0001
Row 6					
0nM estrogen vs. 0.01nM estrogen	-9234	-14115 to -4354	Yes	****	<0.0001
0nM estrogen vs. 1nM estrogen	-14321	-19202 to -9441	Yes	****	<0.0001
0nM estrogen vs. 100nM estrogen	-6185	-11066 to -1305	Yes	**	0.0087

Similar to metabolic activity, the cell number was evaluated in 2D culture, see Figure 8. Donors from separate experiments were averaged together. In general, 100 nM estrogen appears to result in the greatest number of cells compared to the other concentrations of estrogen. Regarding the responses of individual donors, the cell count was highest at 0.01 nM estrogen for Donor 003-2016 (Fig. 21). In contrast, the cell counts for the other estrogen concentrations were similar and all below the concentration of 0.01 nM. Donor 011-2016 had the highest cell count with a concentration of 100 nM estrogen, whereas the lowest count was observed with a concentration of 0.01 nM (Fig 22). The cell count concentrations of Donor 037-2018 steadily increased over time (Fig. 23). Additionally, Donors 7782 and 7783 showed relatively similar cell counts to each other throughout the experiment (Fig. 24, 25). The data of Donor 7784 was omitted due to

technical lab errors producing two days of data with only the 1st data point being valid (Fig. 26). A two-way ANOVA was performed (GraphPad Prism), interaction, day, and dose were significant with *p* values of < 0.0001, < 0.0001, and 0.0030, respectively. A Dunnett's post-hoc test was also conducted (Table 4). Only day 4 and 7 indicated significantly lower cell numbers at 1 nM (day 4) and 100 nM (day 7) estrogen concentrations when compared to 0 nM estrogen. Individual donor graphs for nuclei labeling can be viewed in Appendix B.

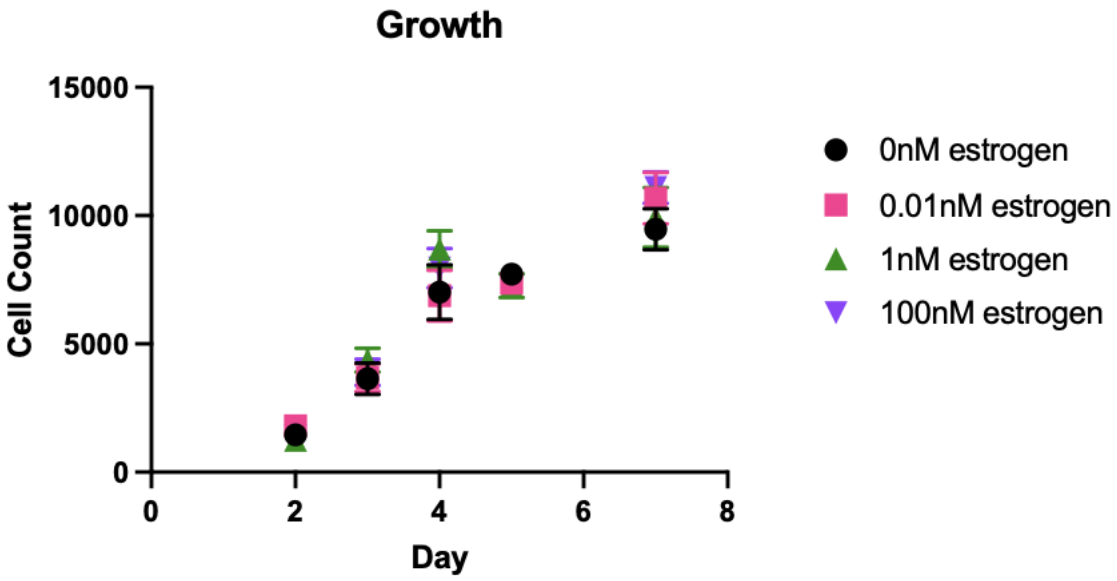

Figure 8 - Cell Expansion Rate in 2D culture Donor Average. (Donors: 003-2016, 011-2016, 037-2018, 7782, 7783) (Replicates per donor: ≥ 6)

Table 4 - Cell Expansion Rate Donor Average Post-hoc Test Results. Rows 1, 2, 3, 4, and 5 represent days 2, 3, 4, 5, and 7, respectively. Row 3 and 5 (Day 4 and 7) indicate significant results for 0 nM estrogen vs 1 nM estrogen (p = 0.0137) and 0 nM estrogen vs 100 nM estrogen (p = 0.0030).

Dunnett's multiple comparisons test	Mean Diff.	95.00% CI of diff.	Below threshold?	Summary	Adjusted P Value
Row 1					
0nM estrogen vs. 0.01nM estrogen	-345.2	-710.8 to 20.45	No	ns	0.0653
0nM estrogen vs. 1nM estrogen	212.0	-79.82 to 503.7	No	ns	0.1796
0nM estrogen vs. 100nM estrogen	42.71	-387.5 to 472.9	No	ns	0.9860
Row 2					
0nM estrogen vs. 0.01nM estrogen	-30.70	-828.5 to 767.1	No	ns	0.9992
0nM estrogen vs. 1nM estrogen	-721.9	-1449 to 5.458	No	ns	0.0518
0nM estrogen vs. 100nM estrogen	-242.2	-992.1 to 507.8	No	ns	0.7340
Row 3					
0nM estrogen vs. 0.01nM estrogen	132.7	-1293 to 1558	No	ns	0.9888
0nM estrogen vs. 1nM estrogen	-1681	-2991 to -371.0	Yes	*	0.0137
0nM estrogen vs. 100nM estrogen	-946.5	-2343 to 449.9	No	ns	0.2101
Row 4					
0nM estrogen vs. 0.01nM estrogen	359.1	-75.39 to 793.6	No	ns	0.1132
0nM estrogen vs. 1nM estrogen	450.6	-58.77 to 960.0	No	ns	0.0855
0nM estrogen vs. 100nM estrogen	386.7	-19.11 to 792.5	No	ns	0.0628
Row 5					
0nM estrogen vs. 0.01nM estrogen	-1207	-2445 to 31.08	No	ns	0.0564
0nM estrogen vs. 1nM estrogen	-463.2	-1922 to 995.7	No	ns	0.7217
0nM estrogen vs. 100nM estrogen	-1623	-2635 to -611.7	Yes	**	0.0030

3.2 Determine the Effect of Estrogen Supplementation on Chondrocyte Extracellular Matrix Production

Aggregate sizes were analyzed throughout the 3-week assay using ImageJ (*Figure 9)*. Aggregate size typically gives a good estimate of the extracellular matrix production of the chondrocytes due to increased ECM (Extracellular Matrix) rather than an increase in cell number. Aggregate initial size was variable based on donor. Overall, aggregate size increased until the plate is treated with IL-1β on day 10. Individually, Donor 003-2016 indicated that 100nM in the presence of IL-1β induces the highest protection on the extracellular matrix from degradation (Fig. 10). Donors 011-2016 and 037-2018 indicate that in the presence of IL-1β, the highest level

of protection from ECM degradation stimulated by inflammatory signaling due to exposure to IL-1β is achieved with a concentration of 0.01 nM (Fig. 27, 28). Aggregate size in Donor 7782 did not exhibit much variation; however, the least ECM protection occurred within the 100 nM estrogen group (Fig. 29). Within Donor 7783, 1 nM estrogen had the highest ECM protection level (Fig. 30). Individual donor graphs of aggregate size can be viewed in Appendix C.

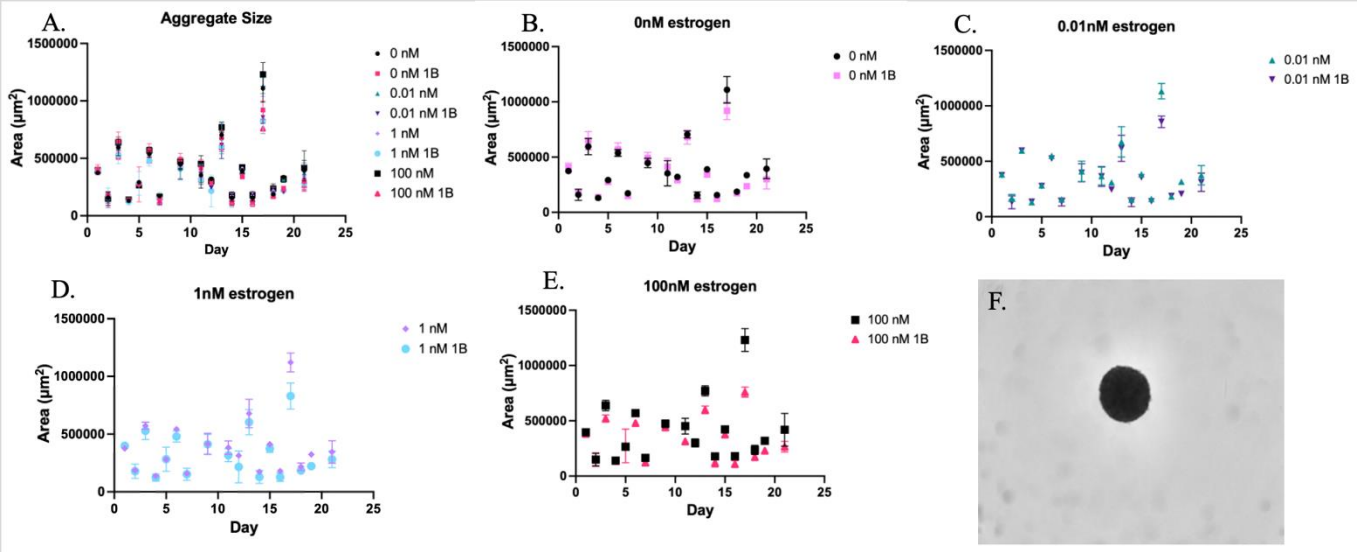

Figure 9 - 22-day Culture Cartilage Aggregate Size Analysis Donor Average. The graphs above represent each donor's aggregate size averages (A), 0 nM estrogen donor aggregate average (B), 0.01 nM estrogen donor aggregate average (C), 1 nM estrogen donor aggregate average (D), 100 nM estrogen donor aggregate average (E), and an aggregate image example used for analysis within the ImageJ program (F). 1B represents samples treated with estrogen and IL-1β. (Donors: 003-2016, 037-2018, 011-2016, 7782, 7783, 7784, Replicates per donor: ≥ 7)

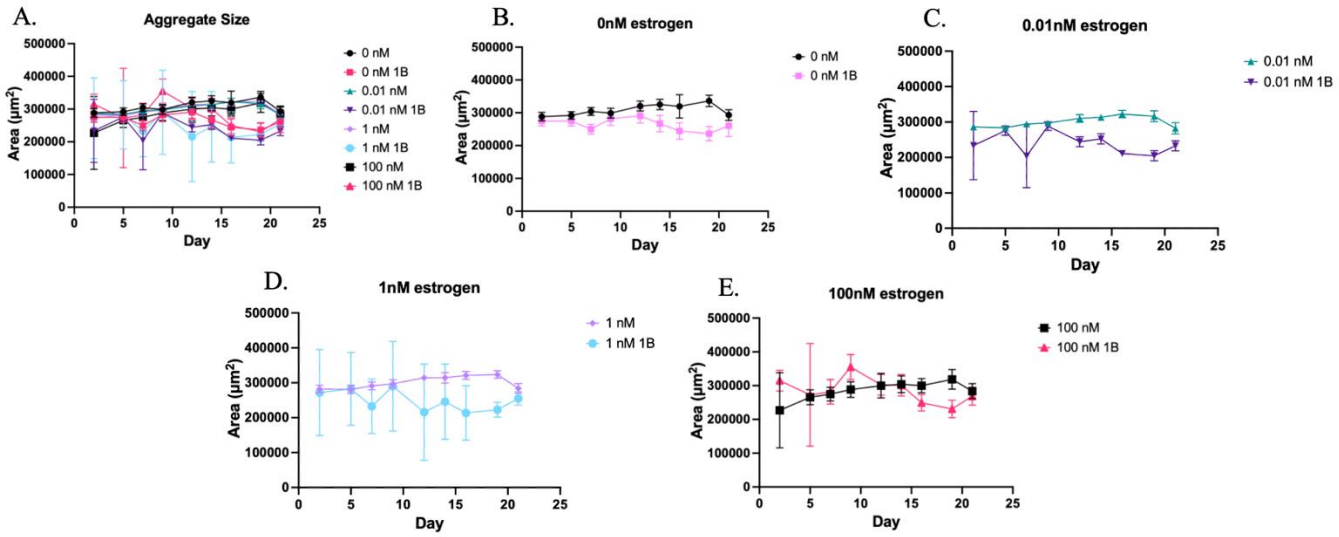

Figure 10 - 22-day Culture Cartilage Aggregate Size Analysis. The graphs above represent each donor's aggregate size averages (A), 0 nM estrogen donor aggregate average (B), 0.01 nM estrogen donor aggregate average (C), 1 nM estrogen donor aggregate average (D), 100 nM estrogen donor aggregate average (E). 1B represents samples treated with estrogen and IL-1β. (Donor 003-2016, Replicates: ≥ 5)

To identify glycosaminoglycan deposition patterns, safranin-o staining was performed (Figure 11). Donor 003-2016 aggregates treated with IL-1β exhibited increased glycosaminoglycan staining when compared to samples without IL-1β; however, there is minimal GAG staining between estrogen concentrations. After the first donor, TGFβ1 was added into the chondrogenic media following experiment one which minimally improved cell differentiation, see Figure 12. Donor 037-2018 produced comparable results for all concentrations of estrogen assessed and no significant positive staining (Fig. 32). The most intense glycosaminoglycan staining in Donor 7782 was observed within the 0.01 nM with IL-1β and the 100 nM without IL-1β groups (Fig. 11). In Donor 7783, the most intense staining for glycosaminoglycan was observed in the estrogen concentration of 0.01 nM with IL-1β (Fig. 34). Individual donor graphs of safranin-o staining can be viewed in Appendix D.

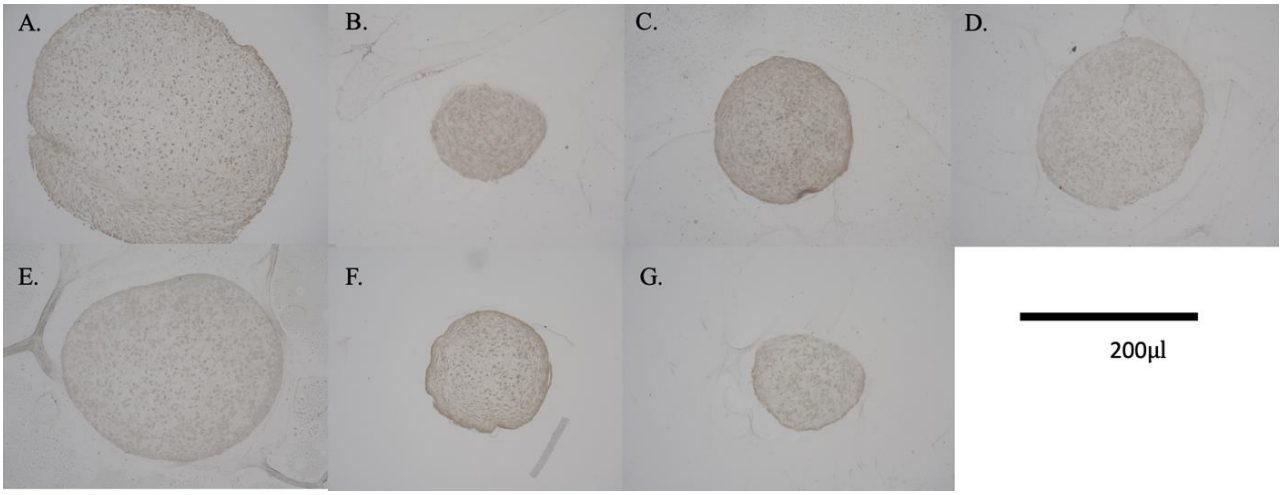

Figure 11 - Glycosaminoglycan Staining of Cartilage Aggregates. Safranin-O (glycoaminoglycan = red)/Fast green (cytoplasm/ECM counterstain = green)/Hematoxylin (nuclei = blue/black) staining of control and estrogen conditions of cartilage aggregates after 3-week culture. E2 = estradiol at 0.01, 1, 100 nM concentrations. The micrographs above show the stained control (A), 0 nM without IL-1β (B), 0.01 nM without IL-1β (C), 0.01 nM with IL-1β (D), 1 nM with IL-1β (E), 100 nM without IL-1β (F), and 100 nM with IL-1β (G). (Donor 7782)

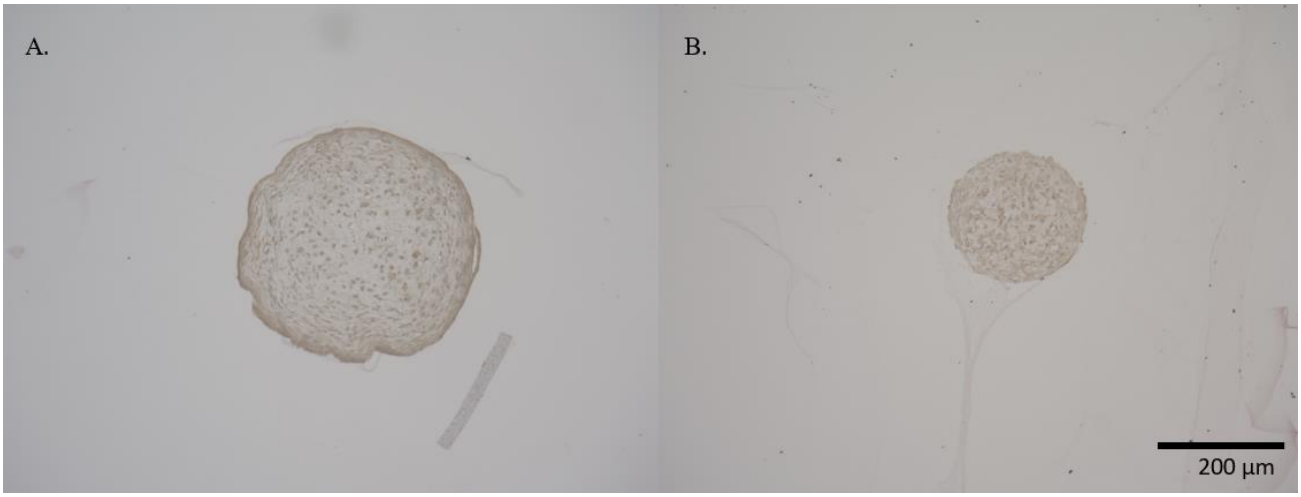

Figure 12 - Example of TGFβ1 Safranin-O Staining. The above micrographs show two 100 nM estrogen samples with no IL1B sample, both of which are treated with TGFβ1. (A) is a sample from donor 037-2018, (B) is a sample from donor 7783.

Additionally, immunohistochemistry was conducted for the purpose of ECM observation in relation to type II collagen deposition, see Figure 13. Donor 003-2016 exhibited some staining for type II collagen when exposed to estrogen concentrations of 0.01 nM with IL-1β, 1 nM

without IL-1β, and 100 nM without IL-1β, although the staining was minimal (Fig. 35). All samples collected from Donor 7782 were negative for type II collagen staining (Fig. 36). Contrarily, in Donor 7783, the 100 nM IL-1β group was observed to produce positive type II collagen staining (Fig. 37). Individual donor graphs of immunohistochemistry staining can be viewed in Appendix E.

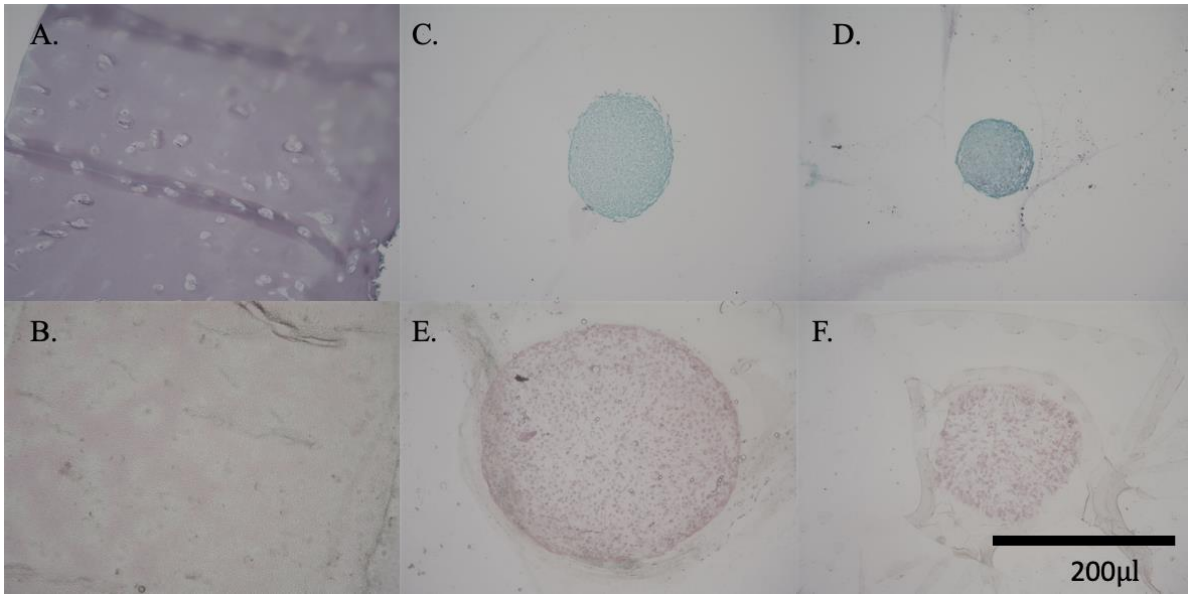

Figure 13 - Type II Collagen Immunohistochemistry Staining of Cartilage Aggregates. The photo above compares two donors (C/D: 003-2016, E/F: 7783) with (A) and (B) representing the control for each donor, respectively. (C) and (E) represent 100 nM estrogen without 1B, (D) and (F) represent 100 nM estrogen with IL-*1β*. The difference between the donors is (C) does not have positive type II collagen staining while (D) has minimal type II collagen staining. (E) and (F) are similar to their control (B). This indicates that the E. and F. are positive for type II collagen staining.

Biochemical assays for glycosaminoglycan, DNA and collagen were also performed. The GAG assay indicates IL-1β has an effect overall on the extracellular matrix with evident decreases in GAG concentrations, particularly in Donor 7783 (Fig. 14). The data from one donor was successfully analyzed in the HDP assay hence there is an obvious lack of comparison between donors. However, 0 nM and 100 nM have significantly more collagen compared to the other estrogen concentrations. Additionally, there is a clear decrease in collagen within the groups

treated with IL-1β (Fig. 15). Some values were excluded as they were below the threshold of a 0 control.

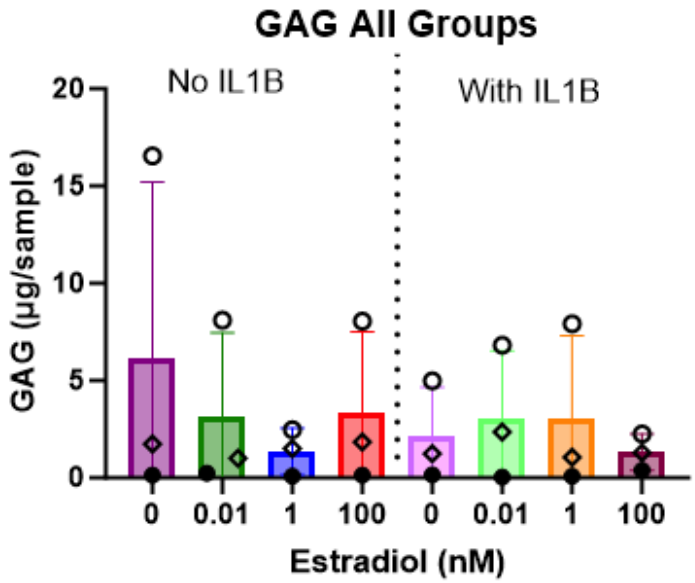

Figure 14 - Glycosaminoglycan Content Analysis by Biochemical Assay. Glycosaminoglycan for each assessed donor is represented by a symbol: ○ = 7783, ◇ = 003-2016. Aggregates cultured without IL-1β are shown to the left, while aggregates cultured with IL-1β are shown to the right. (Replicates per donor: 4)

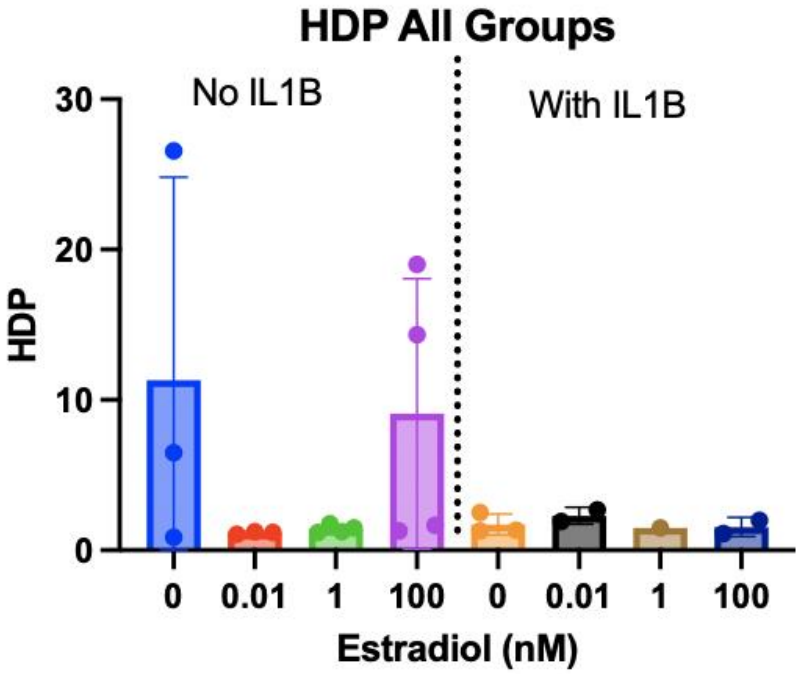

Figure 15 - Aggregate Hydroxyproline (Total Collagen) Content Assessment by Biochemical Analysis. Aggregates cultured without IL-1β are shown to the left, while aggregates cultured with IL-1β are shown to the right. Each • represents a replicate. (Donor: 003-2016)

4. DISCUSSION

4.1 The Effect of Estrogen Supplementation *In Vitro* on Human Chondrocyte Metabolism and Proliferation

According to the resazurin data, the highest metabolic activity overall was observed within the 1 nM estrogen group on day 9 (Figure 7). However, upon assessment of individual donors, the data indicates that among the healthy talus samples (Donor 7782), the 0.01 nM estrogen concentration resulted in the highest metabolic activity, whereas the 0 nM concentration exhibited the lowest activity (Appendix A, Fig. 19). This difference (0 nM vs. 0.01 nM) was considered significant on day six by two-way ANOVA ($p < 0.0001$). Two cryopreserved osteoarthritic donors (003-2016, 011-2016) resulted in 0 nM estrogen producing the highest metabolic activity (Appendix A, Figs. 16 and 17). Donor 037, resulted in 1nM estrogen producing the highest metabolic activity (Appendix A, Fig. 18). Overall, the donors produced varied results upon analyzing the resazurin data which may provide evidence that cartilage responses depend on the pre-existing cartilage condition of the donor.

The data collected from the Hoechst experiment indicated each estrogen level had a similar trend (Figure 8). Overall, the estrogen concentration of 0.01 nM produced the highest cell count whereas 0 nM and 100 nM produced the lowest. However, individual donors produced varied results. Donors 7782 and 7783 have similar cell counts over time (Figs. 24 & 25). We suggest this could be explained due to the donors being closer in age (56 and 51) hence the chondrocytes may respond similarly. In Donors 003-2016 and 011-2016, the cell counts increase over time as

expected and then proceeds to plateau. As the cells expand, the wells can become filled, and proliferation can cease due to contact inhibition within the well.

Previous literature suggests estrogen receptors are more highly expressed in men than women [30]. Considering our metabolic activity and cell count results, there might be a correlation between arthritic samples and the expression of estrogen receptors. In other words, it is possible that osteoarthritic cartilage may have lower estrogen receptor expression than healthy cartilage and thus produce lower metabolic activity stimulation.

For the metabolic activity and cell proliferation experiments, obvious outliers were removed, those being the outer wells due to evident media evaporation. This "edge effect" can be reduced by having a randomized plate, however, plate randomization creates analysis and human error issues which were considered to be more of a concern. Even with these data points omitted, there are still 6 replicates in each donor assessed. Although a non-randomized plate makes the experiments easier, the edge effect occurs as the edge rows (wells A & H) will have decreased fluorescence due to media evaporating. The edge effect was more prominent in our resazurin and Hoechst experiments because PBS was not added to the outer wells as it was thought that evaporation would not be an issue over a 1-week experiment. However, the limitation of the edge effect was reduced in our aggregate size experiment through adding PBS to the unused outer wells.

4.2 Effect of Estrogen Supplementation on Chondrocyte Extracellular Matrix Production

Aggregate sizes were assessed throughout the 3-week assay (Figure 9). Before day 10 with the addition of IL-1β, the aggregate sizes are similar. Our results suggest overall that estrogen in the

presence of IL-1β likely does not affect pellet area. Individual donors provided some variability within the data here as well. Donor 003-2016 indicated 100 nM in the presence of IL-1β provided the most protection (Fig. 10), while some of the other donors indicated 0.01 nM to have the highest protection (Appendix C, Fig. 27, 28, and 31). Overall, estrogen's effect on the ECM seems minimal despite some donor variability.

Neither histological assessment of glycosaminoglycan nor type II collagen staining produced a clear trend, which contradicts our hypothesis that in the presence of estrogen the extra-cellular matrix would be protected. Donors 003-2016 and 7783 resulted in all estrogen concentrations containing IL-1β producing the most intense positive staining, which was unexpected and does not correlate with biochemical assay results. Following experiment one, TGFβ1 was added in the hopes to improve GAG and type II collagen staining; however, each sample indicated minimal staining (Figure 11). Normal human chondrogenesis requires TGFβ1 to stimulate GAG and type II collagen [35, 36, 43, 44]. The first experiment was performed to see if E2 could produce this ECM stimulation effect in isolation. The glycosaminoglycan staining results from the safranin-o experiment suggest differing estrogen levels do not heavily influence GAG deposition, hence have minimal effect on cartilage extra-cellular matrix.

Upon the analysis of the biochemical data, in the presence of IL-1β there is a significant decrease in GAG levels, especially in 100 nM estrogen. In both donors assessed (003-2016 and 7783), 0.01 nM seemed to produce more GAG when treated with IL-1β. Donor 003-2016 produced significantly lower GAG levels when compared to 7783. This may be due to Donor 003-2016

already being osteoarthritic, while Donor 7783 is healthy cartilage. As only two donors were successfully analyzed, there is not enough data to suggest a clear answer on whether the ECM is affected by differing estrogen concentrations.

In our HDP assay which assessed total collagen, some replicates produced more collagen especially in 0 nM and 100 nM estrogen. However, 003-2016 was the only donor that was able to be analyzed for HDP and did not produce positive type II collagen immunohistochemistry staining. We can possibly infer from this that the HDP assay reflects both fibrotic cartilage (type I collagen) and hyaline cartilage (type II collagen). Overall, our DNA biochemical assay data was determined unreliable for all six donors because so many of our samples were below the standard curve. The reason for this could be the adoption of a different Papain supplier as a result of COVID-19, which may possess DNAse properties leading to the breakdown of DNA. In addition, our samples were melted in the bead bath for several of our donors due to a temperature malfunction, hence the lack of DNA biochemistry data.

Overall, there was minimal change in most donors and the effects were inconsistent. It seems that estrogen minimally affects ECM production, protection from inflammatory challenge (IL-1β) and proliferation *in vitro*. However, by using an *in vitro* model, there are many components missing that relate to the complex physiology of the joint. For example, in the human body estrogen fluctuates throughout a woman's life and estrous cycle; however, in our experiment we treated the samples with the same concentrations over 22 days which is not representative of natural physiology. Different donor plates were also not imaged on the same day leading to

unclear data graphs when averaged together. Additionally, there were individual donor variations which could be explained by the health of the tissue at the time of culture, frozen versus fresh, age, race, or even arthritis family history. Some of these aspects such as family history were not known in this experiment thus cannot be compared or concluded to be definite factors affecting donor variation.

4.3 Future Studies

Our biochemical assay data was determined unreliable due to the potential use of a DNase active papain. In future research, the potential DNase activity of the papain could be explored which could improve biochemical data in prospective studies. In addition, two types of cartilage were utilized in this study (Table 1). Analyzing the potential contrasting reactions of healthy cartilage and osteoarthritic cartilage may provide a better understanding of the variations observed within our donor samples. Osteoarthritic samples may have less estrogen receptor expression, leading to a decrease in estrogen binding. Future studies could conduct flow cytometry experiments and compare estrogen receptor expression in healthy and osteoarthritic samples. This may give potential insight into whether there is a difference in estrogen receptor expression. Our proliferation and metabolic activity experiment samples were not treated with IL-1β. Future studies could perform a similar experiment and treat some of the wells with IL-1β. This would provide additional information on the potential impact of IL-1β treatment on proliferation and metabolic activity. Additionally, researching the various components of the joint and investigating their response to estrogen, such as the synovium or subchondral bone, may provide a deeper understanding of the overall mechanism of ERT in protecting the joint. Finally, we treated the aggregates with IL-1β; however, we did not add immune cells. Subsequent investigations may consider conducting a similar method involving IL-1β and adding monocytes. This may allow for a more natural physiologically related system and improve our *in vitro* model.

5. CONCLUSION

Estrogen concentrations representing normal adult, pregnant and post-menopausal concentrations did not have a large or consistent effect on cartilage extra-cellular matrix production, protection from inflammatory degradation, or proliferation. Our results suggest a donor dependent effect of estrogen and IL-1β. This offers significant understanding of how cartilage might respond differently based on its pre-existing condition in the body when studied *in vitro*.

APPENDIX A

Breakdown of Metabolic Activity Data per Donor

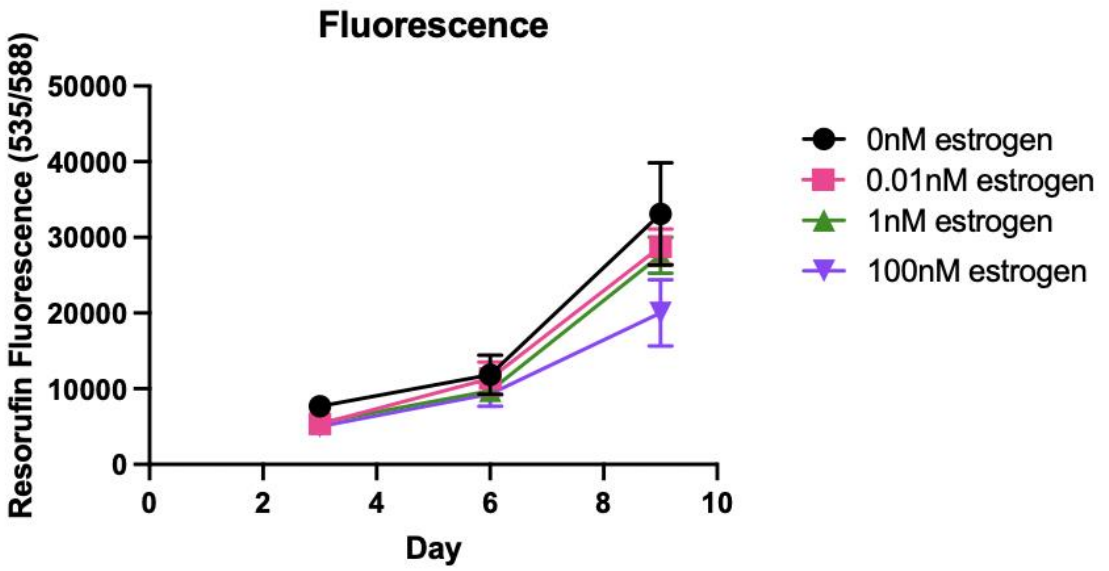

Figure 16 - Metabolic Activity of Chondrocytes During 2D Expansion. Donor: 003-2016, Replicates: ≥ 6.

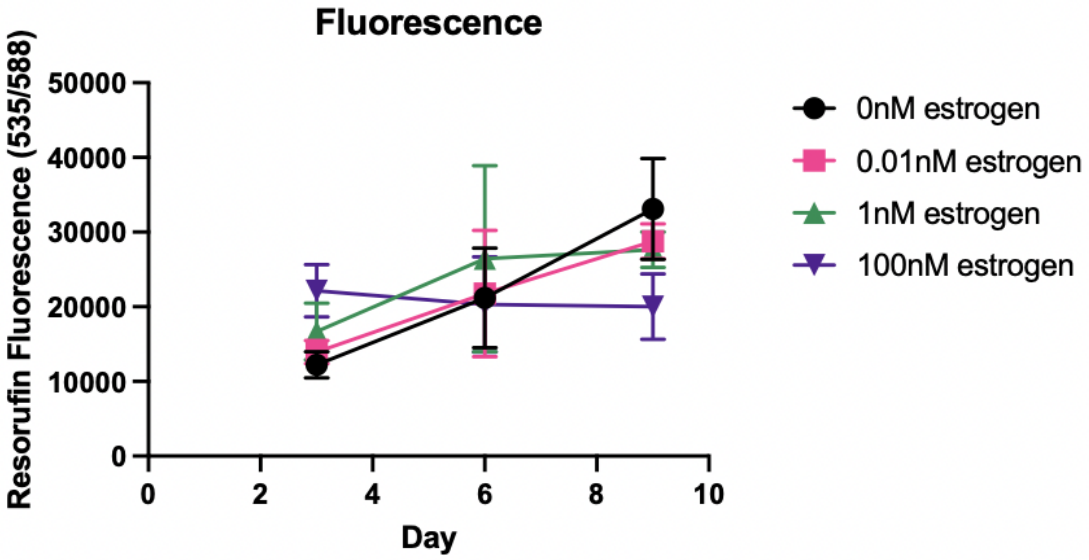

Figure 17 - Metabolic Activity of Chondrocytes During 2D Expansion. Donor: 011-2016, Replicates: ≥ 6.

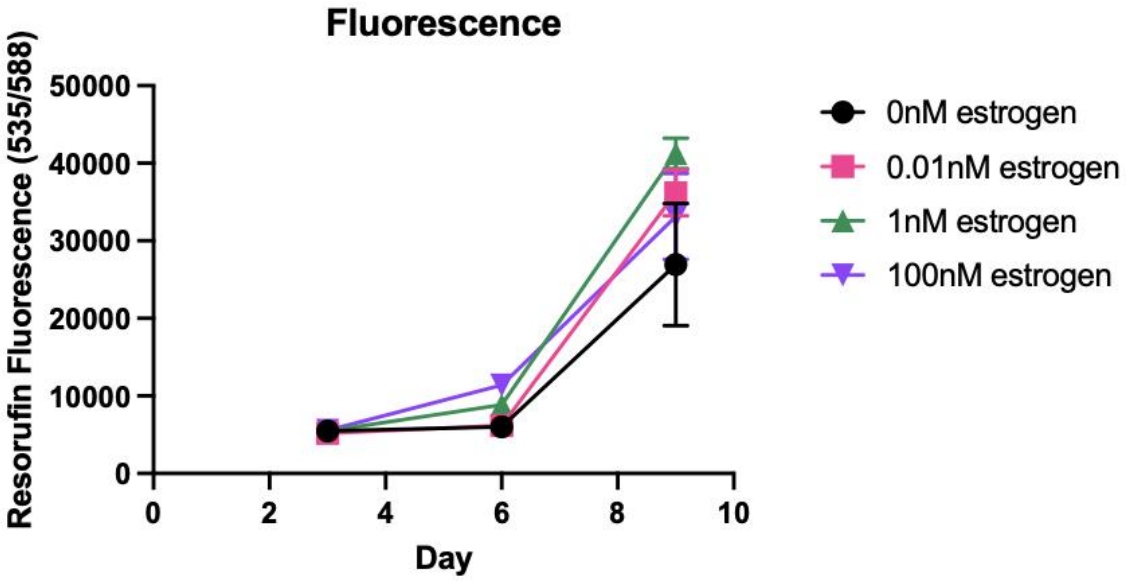

Figure 18 - Metabolic Activity of Chondrocytes During 2D Expansion. Donor: 037-2018, Replicates: ≥ 6.

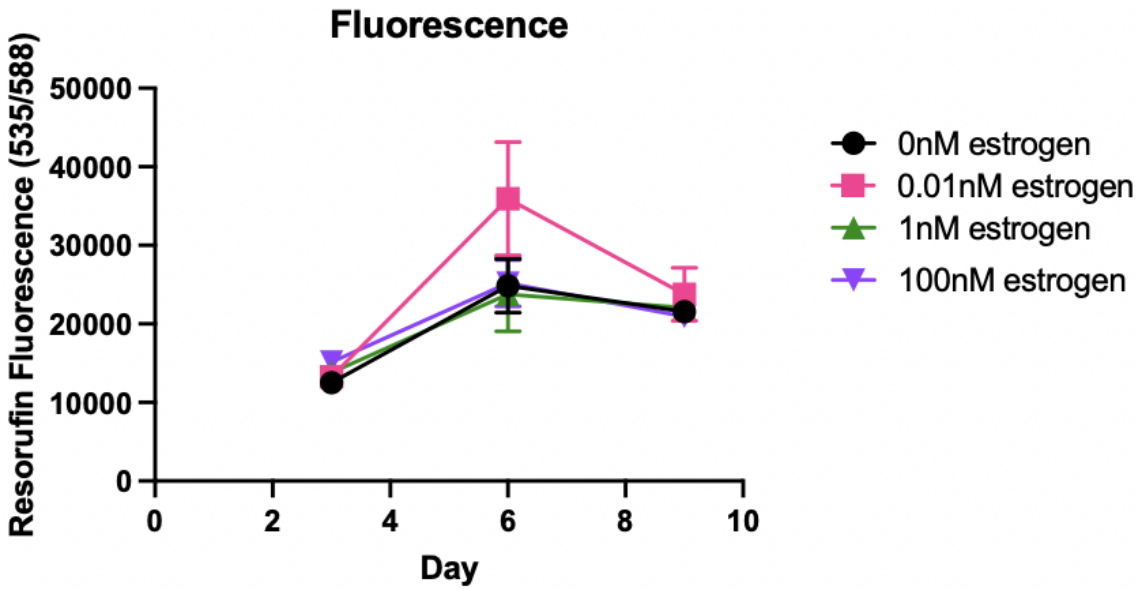

Figure 19 - Metabolic Activity of Chondrocytes During 2D Expansion. A Dunnet post-hoc test was indicated day six was significant when 0 nM was compared to 0.01 nM estrogen ($p < 0.0001$). Donor: 7782, Replicates: ≥ 6.

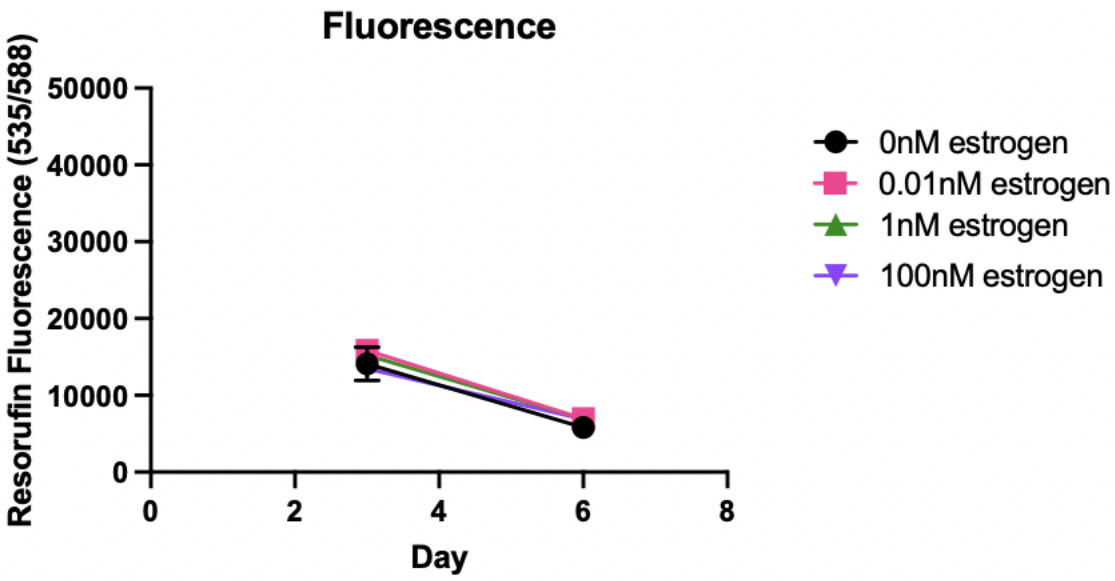

Figure 20 - Metabolic Activity of Chondrocytes During 2D Expansion. The donor represented in the graph above was excluded due to lab errors resulting in two days of data instead of three. Donor 7784, Replicates: ≥ 6.

APPENDIX B

Breakdown of Hoechst Nuclei Labeling Data per Donor

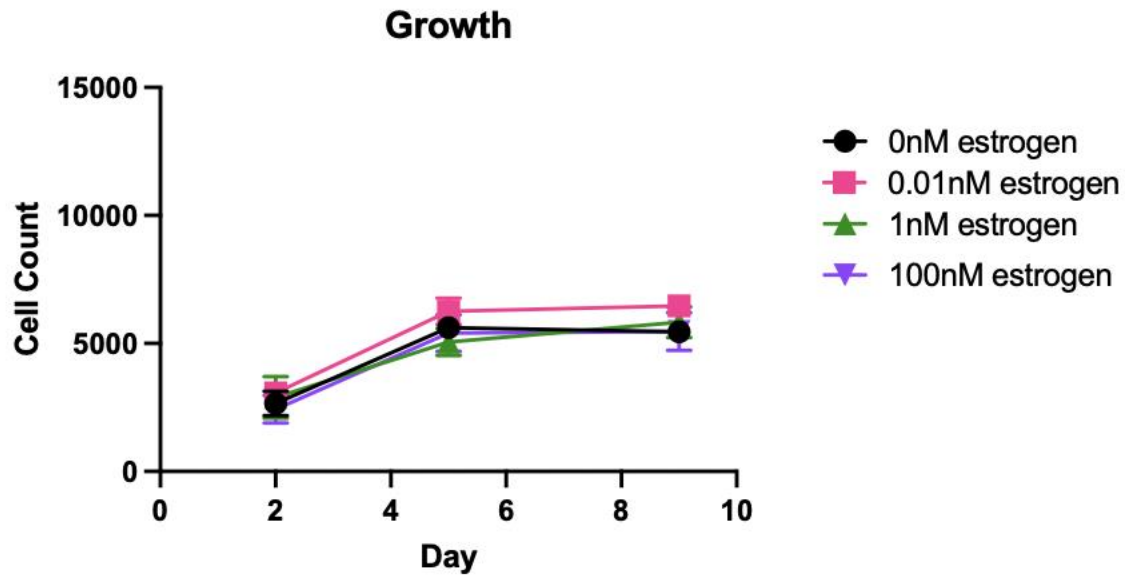

Figure 21 - Hoechst Nuclei Labeling Data. Donor 003-2016, Replicates: ≥ 5.

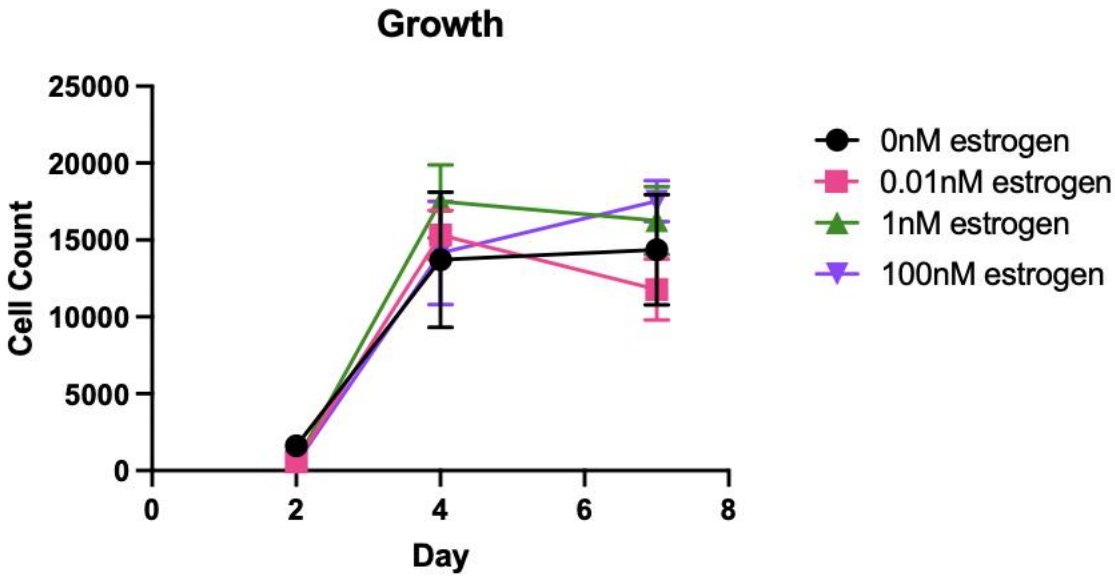

Figure 22 - Hoechst Nuclei Labeling Data. Donor: 011-2016, Replicates: ≥ 5.

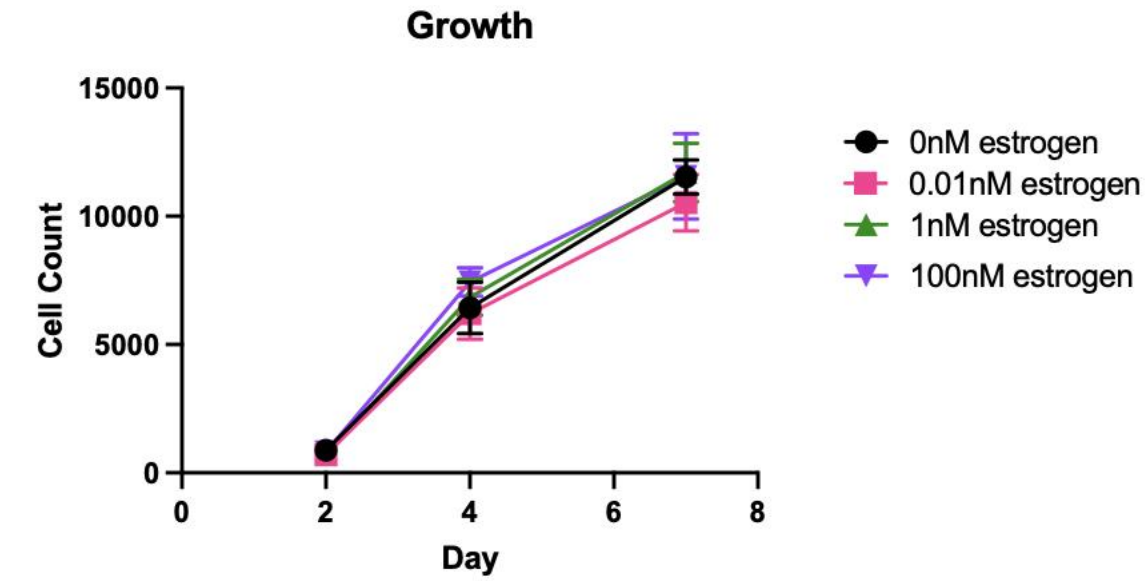

Figure 23 - Hoechst Nuclei Labeling Data. Donor: 037-2018, Replicates: ≥ 5.

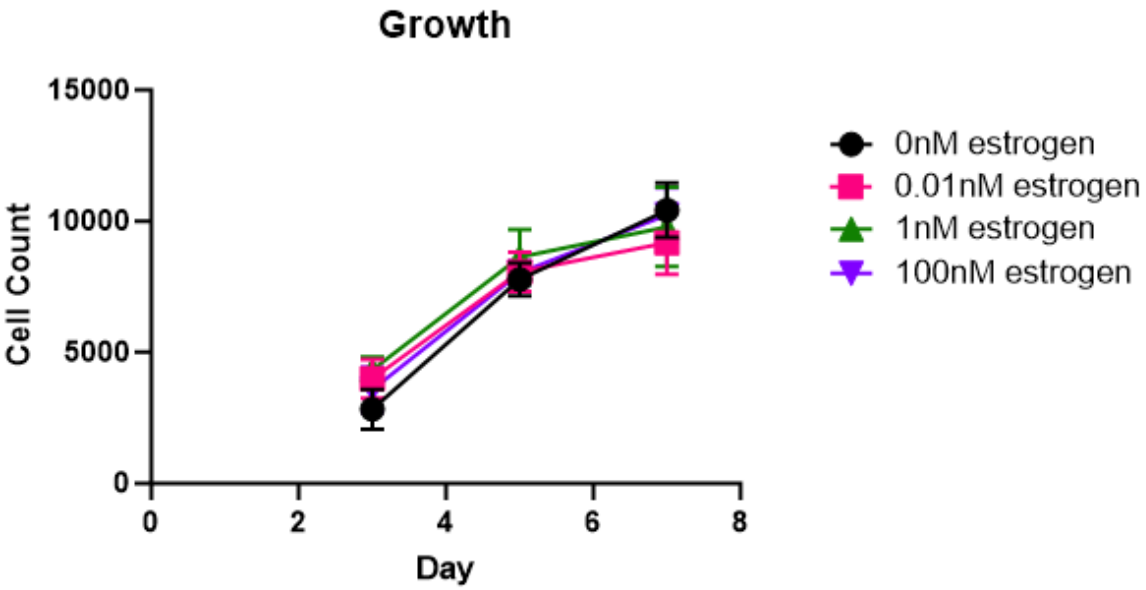

Figure 24 - Hoechst Nuclei Labeling Data. Donor: 7782, Replicates: ≥ 5.

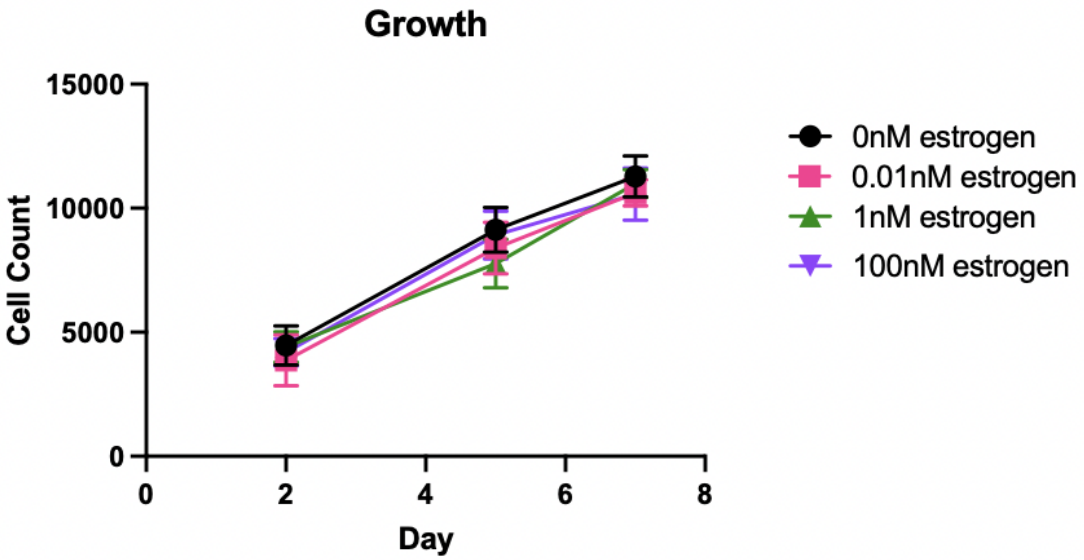

Figure 25 - Hoechst Nuclei Labeling Data. Donor: 7783, Replicates: ≥ 5.

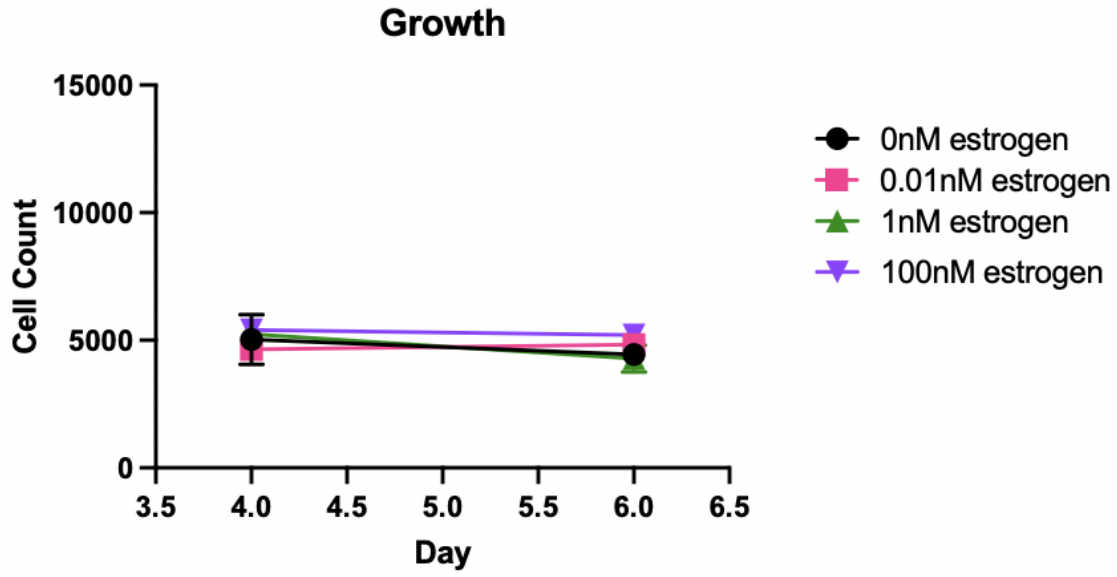

Figure 26 - Hoechst Nuclei Labeling Data. The donor represented in the graph above was excluded due to lab errors resulting in two days of data instead of three. Donor: 7784, Replicates: ≥ 5.

APPENDIX C

Breakdown of Aggregate Size Data per Donor

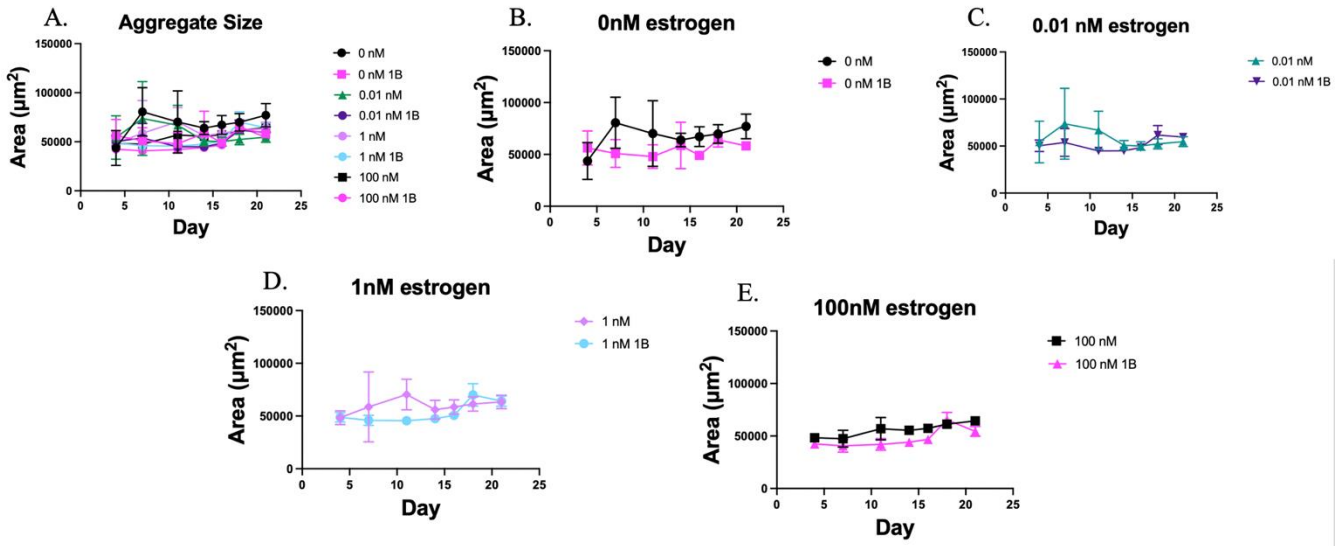

Figure 27 - 22-day culture aggregate size analysis. Donor: 011-2016, Replicates: 7 on Day 0 with some replicates lost over time leaving ≥ 4 on Day 21.

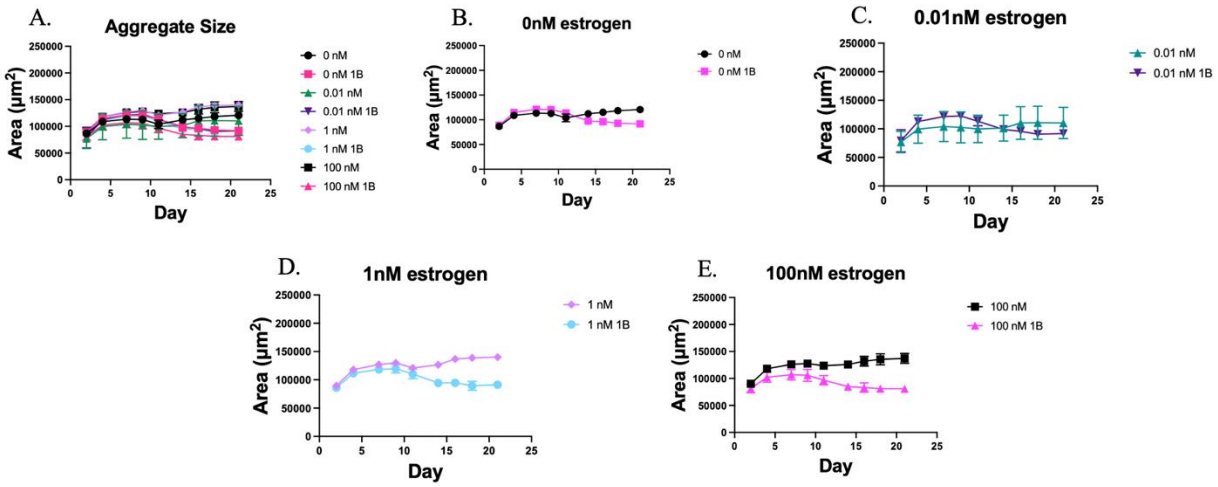

Figure 28 - 22-day culture aggregate size analysis. Within this donor, there is a clear IL-1β response on Day 10 and protection at 0.01 nM estrogen. Donor: 037-2018, Replicates: 7 on Day 0 with some replicates lost over time leaving ≥ 6 on Day 21.

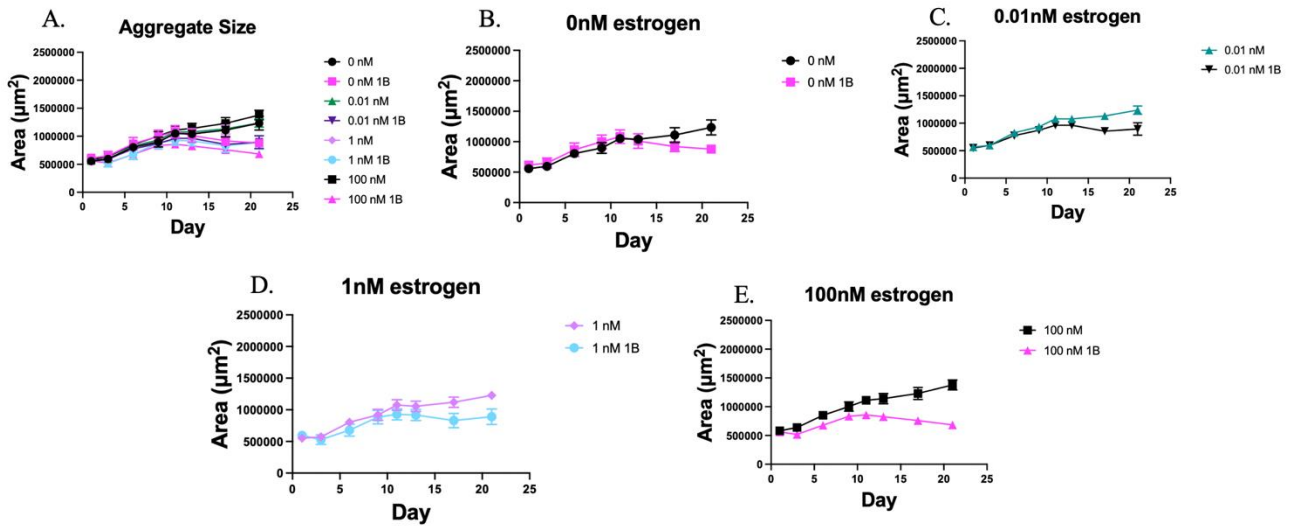

Figure 29 - 22-day culture aggregate size analysis. Donor: 7782, Replicates: 7 on Day 0 with some replicates lost over time leaving ≥ 4 on Day 21.

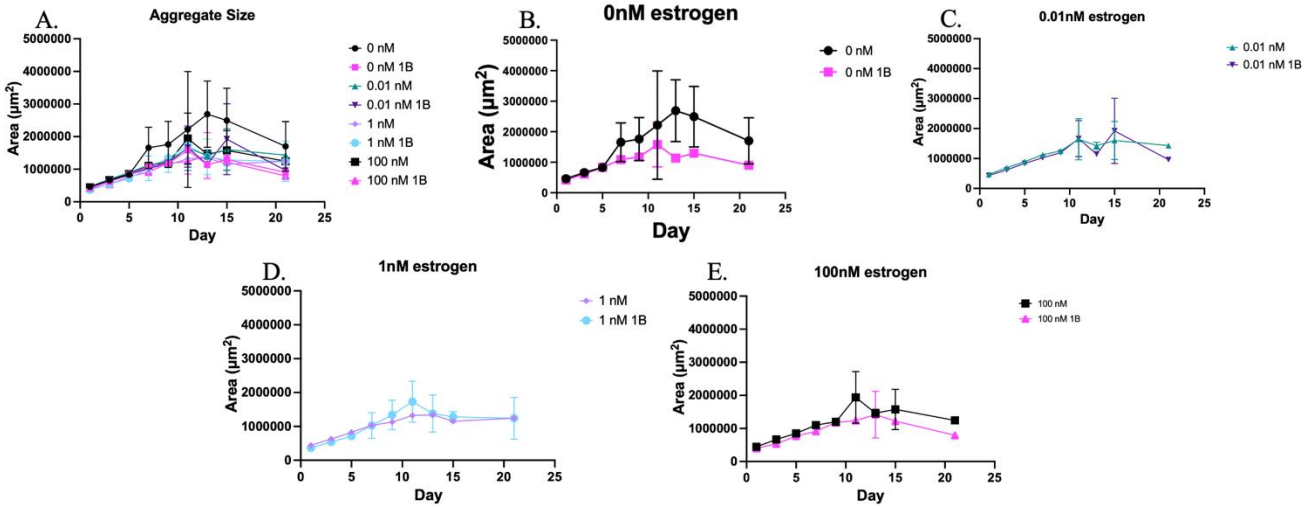

Figure 30 - 22-day culture aggregate size analysis. Donor: 7783, Replicates: 7 on Day 0 with some replicates lost over time leaving ≥ 3 on Day 21.

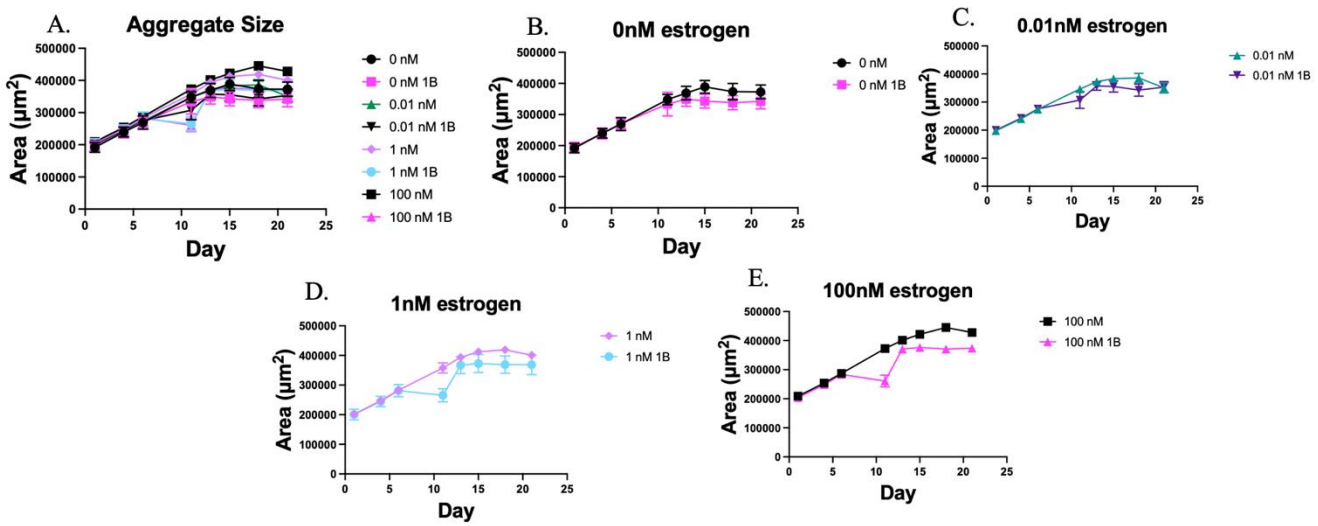

Figure 31 - 22-day culture aggregate size analysis. Donor: 7784, Replicates: 7.

APPENDIX D

Breakdown of Histology Data per Donor

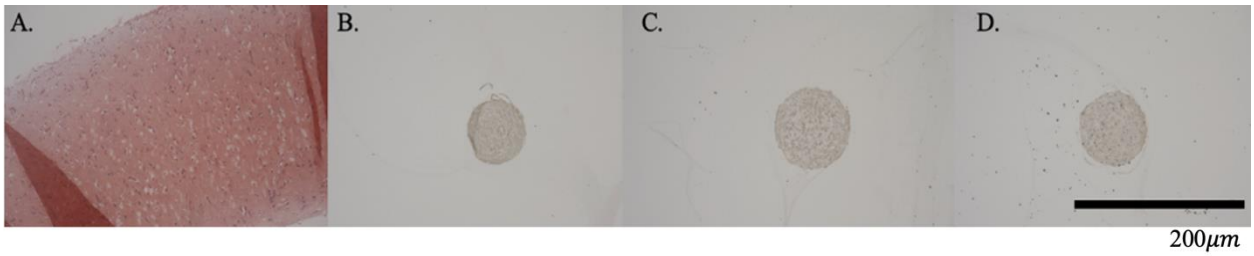

Figure 32 - Glycosaminoglycan Staining of Cartilage Aggregates. The micrographs above show the stained control (A), 0.01 nM without IL-1β (B), 100 nM without IL-1β (C), and 100 nM with IL-1β (D). (Donor 037-2018)

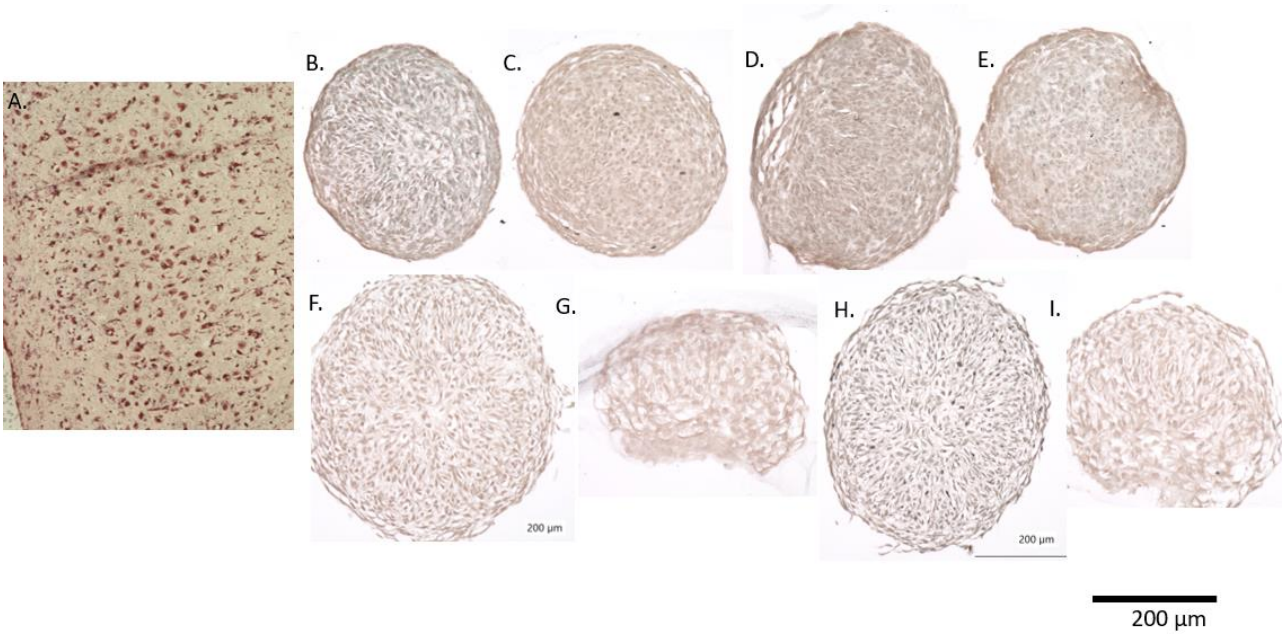

Figure 33 - Glycosaminoglycan Staining of Cartilage Aggregates. The micrographs above show the stained control (A), 0 nM without IL-1β (B), 0.01 nM without IL-1β (C), 0.01 nM with IL-1β (D), 1 nM with IL-1β (E), 100 nM without IL-1β (F), and 100 nM with IL-1β (G). **(**Donor 003-2018)

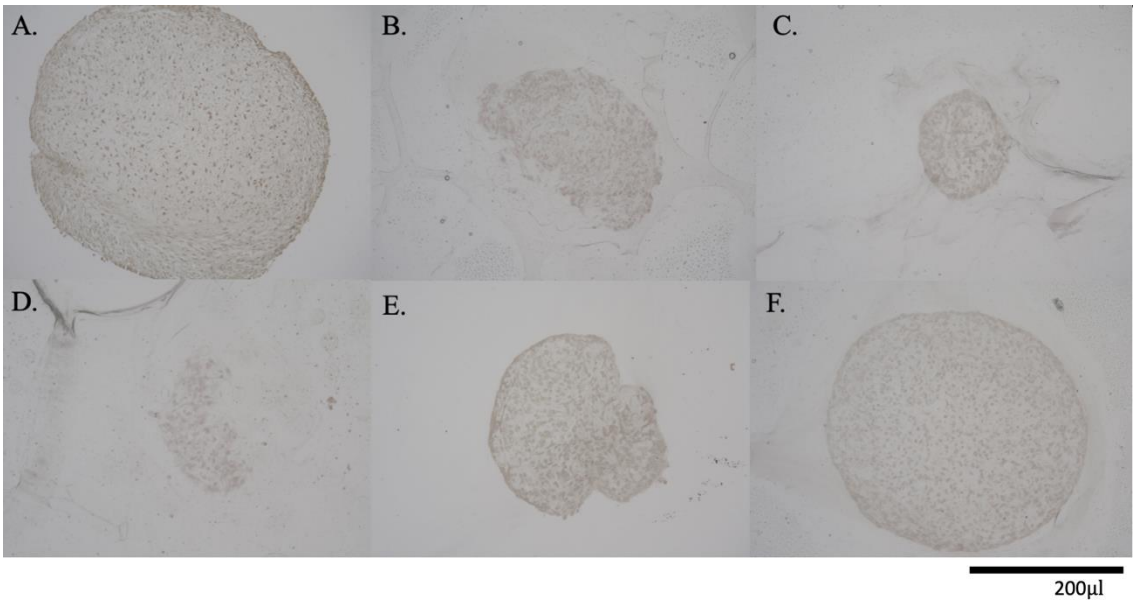

Figure 34 - Glycosaminoglycan staining of cartilage aggregates. The micrographs above show the stained control (A), 0 nM without IL-1β (B), 0 nM with IL-1β (C), 0.01 nM without IL-1β (D), 0.01 nM with IL-1β (E), and 100 nM with IL-1β (F). (Donor 7783)

APPENDIX E

Breakdown of Immunohistochemistry Data per Donor

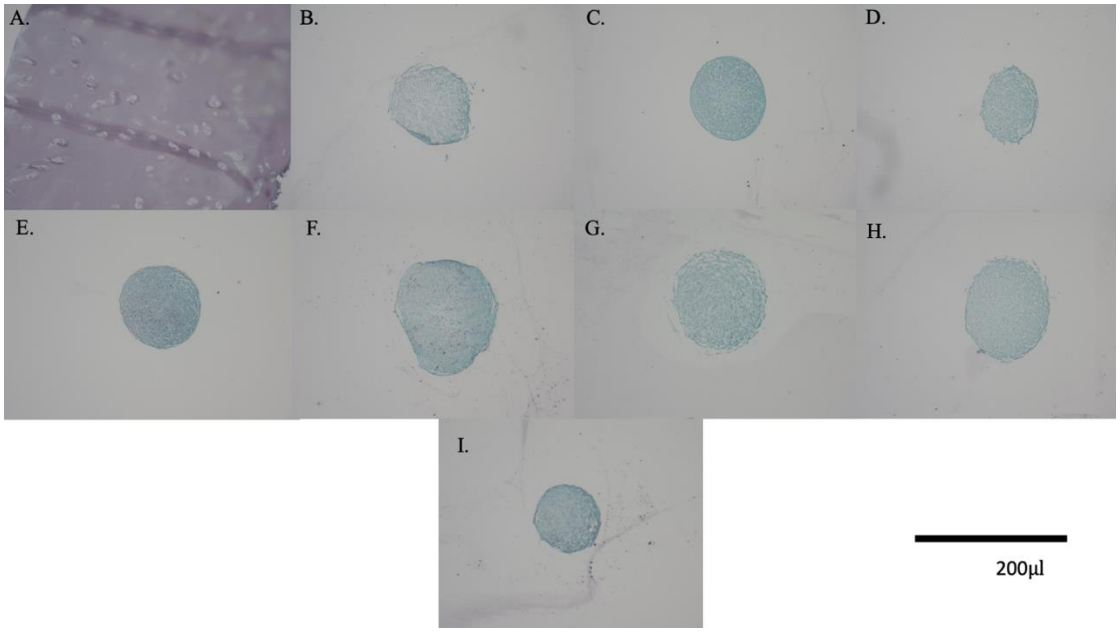

Figure 35 - Type II Collagen Immunohistochemistry Staining of Cartilage Aggregates. The micrographs above show the stained control (A), 0 nM without IL-1β (B), 0 nM with IL-1β (C), 0.01 nM without IL-1β (D), 0.01 nM with IL-1β (E), 1 nM without IL-1β (F), 1 nM with IL-1β (G), 100 nM without IL-1β (H), and 100 nM without IL-1β (I). (Donor 003-2016, TGFβ1 absent)

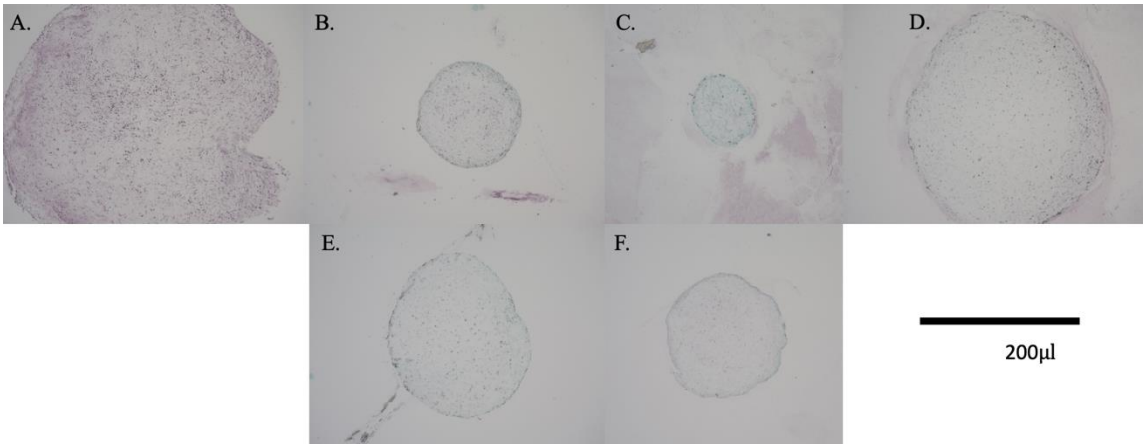

Figure 36 - Type II Collagen Immunohistochemistry Staining of Cartilage Aggregates. The micrographs above show the stained control (A), 0 nM without IL-1β (B), 0 nM with IL-1β (C), 0.01 nM without IL-1β (D), 1 nM with IL-1β (E), 100 nM without IL-1β (F). (Donor 7782)

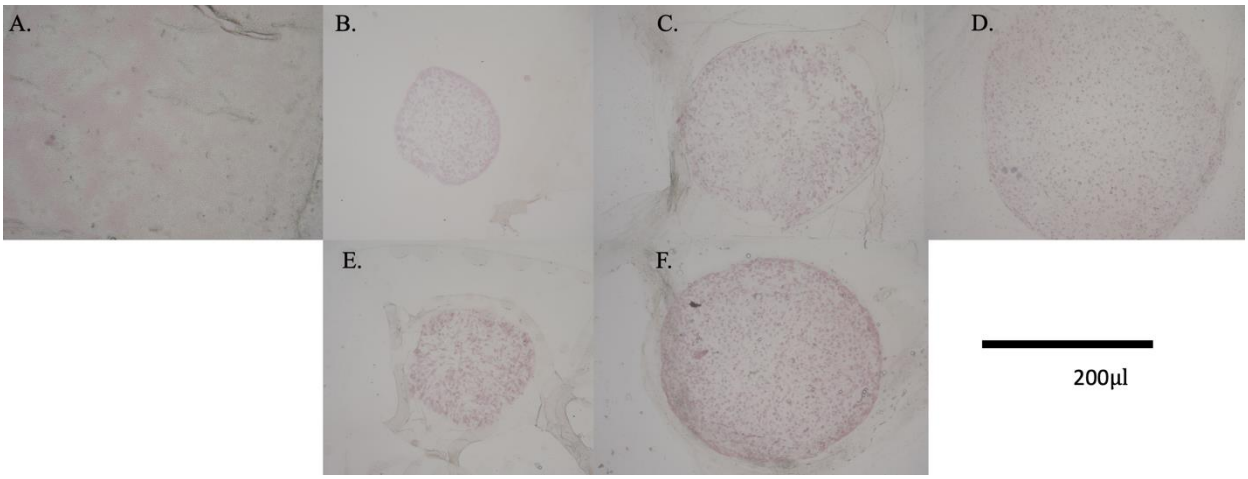

Figure 37 - Type II Collagen Immunohistochemistry Staining of Cartilage Aggregates. The micrographs above show the stained control (A), 0 nM without IL-1β (B), 0.01 nM without IL-1β (C), 0.01 nM with IL-1β (D), 100 nM without IL-1β (E), 100 nM with IL-1β (F). **(**Donor 7783)

REFERENCES

1. Goldring M. B., et al., The control of chondrogenesis. Journal of Cellular Biochemistry, 2005. 97(1): p. 33-44.
2. Goldring M. B., Chondrogenesis, chondrocyte differentiation, and articular cartilage metabolism in health and osteoarthritis. Therapeutic Advances in Musculoskeletal Disease, 2012. 4(4): p. 269-285.
3. Eyre D., Articular cartilage and changes in Arthritis: collagen of articular cartilage. BMC Journal, 2001. 4(30)
4. Martin J. and Buckwalter J., *The Role of Chondrocyte Senescence in the Pathogenesis of Osteoarthritis and in Limiting Cartilage Repair*. The Journal of Bone & Joint Surgery, 2003. **85**(2): p. 106-110.
5. Barbero A., et al., *Age related changes in human articular chondrocyte yield, proliferation and post-expansion chondrogenic capacity*. Osteoarthritis Cartilage, 2004. **12**(6): p. 476-484.
6. Fuentes N. and Silveyra P., *Estrogen receptor signaling mechanisms*. Advances in Protein Chemistry and Structural Biology, 2019. **116**: p. 135-170.
7. Ruggiero R.J. and Likis F.E., *Estrogen: physiology, pharmacology, and formulations for replacement therapy*. J Midwifery Womens Health, 2002. **47**(3): p. 130-138.
8. Razandi M., et al., *Plasma Membrane Estrogen Receptors Exist and Functions as Dimers*. Molecular Endocrinology, 2004. **18**(12): p. 2854-2865.
9. Ushiyama T., et al., *Expression of genes for estrogen receptors α and β in human articular chondrocytes*. Osteoarthritis Cartilage, 1999. **7**(6): p. 560-566
10. Parry T., et al., *Chapter 10- Nuclear Receptors and the Adaptive Response of the Heart*. Endocrinology of the Heart in Health and Disease, 2017. p. 249-284
11. VIVO Pathology. *Gonadotropins: Luteinizing and Follicle Stimulating Hormones*. 2018 [cited 2022 17 October]: Available from: http://www.vivo.colostate.edu/hbooks/pathphys/endocrine/hypopit/lhfsh.html
12. Liu Y., Zhang M., et al., *High follicle-stimulating hormone levels accelerate cartilage damage of knee osteoarthritis in postmenopausal women through PI3K/AKT/NF-κB pathway*. FEBS Open Bio, 2020. **10**(10): p. 2235-2245.
13. Mihm M., et al., *The normal menstrual cycle.* Animal Reproductive Science, 2011. **124**(3-4): p. 229-236.
14. McNamara M., et al., *Perimenopause*. Annals of Internal Medicine, 2015. **162**(3): p. 157-240.
15. Endemann G., Goop. *Menopause and Perimenopause*. 2021 May 3, 2022 [cited 2022 15 October]: Available from: https://goop.com/wellness/health/menopause-and-perimenopause/
16. Santoro N., et al., *The Menopausal Transition: Signs, Symptoms, and Management Options*. The Journal of Clinical Endocrinology & Metabolism, 2021. **106**(1): p. 1-17.
17. Santoro N., et al., *Menstrual Cycle Hormone Changes in Women Traversing Menopause: Study of Women's Health Across the Nation*. The Journal of Clinical Endocrinology & Metabolism, 2017. **102**(2): p. 2218-2229

18. Mayo Clinic. *Menopause*. [cited 2022 15 October]: Available from: **https://www.mayoclinic.org/diseases-conditions/menopause/symptoms-causes/syc-20353397**
19. Harlow S., et al., *Executive Summary of the Stages of Reproductive Aging Workshop + 10: Addressing the Unfinished Agenda of Staging Reproductive Aging*. The Journal of Clinical Endocrinology & Metabolism, 2012. **97**(4): p. 1159-1168.
20. Breu A., et al., *Estrogen reduces cellular aging in human mesenchymal stem cells and chondrocytes.* Journal of Orthopedic Research, 2011. **29**(10): p. 1563-1571.
21. Rousseau M.E., *Evidence-based practice in women's health: hormone replacement therapy for women at menopause*. J Midwifery Womens Health, 2001. **46**(3): p. 167-180.
22. Wluka A.E., et al., *Users of estrogen replacement therapy have more knee cartilage than non-users*. Annals of Rheumatic Diseases, 2001. **60**: p. 332-336
23. Fahad H.S., et al., *Osteoarthritis and the postmenopausal woman: Epidemiological, magnetic resonance imaging, and radiological findings*. Semin Arthritis Rheum., 2004. **34**(3): p. 631-636
24. Cirillo D.J., et al., *Effect of hormone therapy on risk of hip and knee joint replacement in women's health initiative*. Arthritis & Rheumatology, 2006. **54**(10): p. 3194-3204.
25. Hays J., et al., *Effects of Estrogen plus Progestin on Health-Related Quality of Life.* The New England Journal of Medicine, 2003. **387**(21).
26. Liang Y., et al., *E2 regulates MMP-13 via targeting miR-140 in IL-1 β- induced extracellular matrix degradation in human chondrocytes*. BMC Journal, 2016. **18**(105).
27. Dennis J.E., et al., *Physioxia Stimulates Extracellular Matrix Deposition and Increases Mechanical Properties of Human Chondrocyte-Derived Tissue- Engineered Cartilage*. Frontiers in Bioengineering and Biotechnology, 2020. **8**.
28. Martyniak K., Lokshina A., Cruz M.A., Karimzadeh M., Kemp R., Kean T.J., *Biomaterial composition and stiffness as decisive properties of 3D bioprinted constructs for type II collagen stimulation*. Acta Biomater, 2022. **152**: p. 221-234.
29. Riley J. Williams III, MD. Articular Cartilage Injury of the Knee. [cited 2023 1 September]: Available **from: https://rileywilliamsmd.com/articular-cartilage-injury-knee-damage-cartilage-shear-injury-manhattan-new-york-city-ny/#:~:text=Grade%202%20%E2%80%93%20Partial%20thickness%20loss,loss%2C%20subchondral%20bone%20is%20exposed**
30. Santoro N., et al., *The Menopausal Transition: Signs, Symptoms, and Management Options*. The Journal of Clinical Endocrinology & Metabolism, 2021. **106**(1): p. 1-15.
31. Patel J., Chen S., Katzmeyer T., Pei Y., Pei M., *Sex Dependent variation in cartilage adaptation: from degeneration to regeneration*. Biol Sex Differ, 2023. 14.
32. Kinney R.C., Schwartz Z., Week K., Lotz M.K., Boyan B.D., *Human articular chondrocytes exhibit sexual* dimorphism *in their responses to 17β-estradiol*. Osteoarthritis and Cartilage, 2004. **13**(4): p. 330-337
33. Truong R.D., Bernier M.A., Dennis J.E., Kean T.J., *Synoviocyte-Derived Extracellular Matrix and bFGF Speed Human Chondrocyte Proliferation While Maintaining Differentiation Potential*. Frontiers in Bioengineering and Biotechnology, 2022. 10
34. Kean T.J., Dennis J.E., Synoviocyte Derived-Extracellular Matrix Enhances Human Articular Chondrocyte Proliferation and Maintains Re-Differentiation Capacity at Both

Low and Atmospheric Oxygen Tensions. PLoS One. 2015;10(6):e0129961. doi: 10.1371/journal.pone.0129961. PubMed PMID: 26075742; PMCID: 4468209.
35. Chen P., Li B., Ou-Yang L., *Role of estrogen receptors in health and disease*. Front Endocrinol (Lausanne), 2022. 13
36. Vaux D.L., Fidler F., Cumming G., *Replicates and Repeats – what is the difference and is it significant?* EMBO Rep., 2012. **13**(4): p. 291-296
37. Cook J.L., et al., *A novel system improves preservation of osteochondral allographs*. Clinical Orthopedics and Related Research, 2014. **472**(11): p. 3404-14
38. Jensen E.V., Desombre E.R., Kawashima T., Suzuki T., Kyser K., Jungblut P.W., *Estrogen-binding substances of target tissues*. Science, 1967. **158**(3800): p. 529–530
39. Kuiper G.G., Enmark E., Pelto-Huikko M., Nilsson S., Gustafsson J.A., *Cloning of a novel receptor expressed in rat prostate and ovary*. Proc Natl Acad Sci USA, 1996. **93**(12): p. 5925–5930
40. Chubinskaya S., Cotter E.J., Frank R.M., Hakimiyan A.A., Yanke A.B., Cole B.J., *Biological Characteristics of Shoulder Articular Cartilage in Comparison to Knee and Ankle Articular Cartilage From Individual Donors*. Cartilage, 2021. **12**(4): p. 456-467
41. Martyniak K, Lokshina A, Cruz MA, Karimzadeh M, Kemp R, Kean TJ. Biomaterial composition and stiffness as decisive properties of 3D bioprinted constructs for type II collagen stimulation. Acta Biomaterialia. 2022. doi: https://doi.org/10.1016/j.actbio.2022.08.058.
42. Martyniak K, Kennedy S, Karimzadeh M, Cruz MA, Jeon O, Alsberg E, Kean TJ. Optimizing Bioink Composition for Human Chondrocyte Expression of Lubricin. Bioengineering. 2023;10(9):997. PubMed PMID: doi:10.3390/bioengineering10090997.